Katharina Weinzerl, BSc

PMR1 in calcium homeostasis and autophagy

MASTERARBEIT

zur Erlangung des akademischen Grades

Master of Science

Masterstudium Molekulare Mikrobiologie

eingereicht an der

Technischen Universität Graz

Betreuerin

Ass.-Prof. Priv. Doz. Dr. Sabrina Büttner

Institut für molekulare Biowissenschaften

Graz, Juli 2015

EIDESSTATTLICHE ERKLÄRUNG

Ich erkläre an Eides statt, dass ich die vorliegende Arbeit selbstständig verfasst, andere als die angegebenen Quellen/Hilfsmittel nicht benutzt, und die den benutzten Quellen wörtlich und inhaltlich entnommenen Stellen als solche kenntlich gemacht habe. Das in TUGRAZonline hochgeladene Textdokument ist mit der vorliegenden Masterarbeit identisch.

Datum

Unterschrift

Für meine Eltern

Abstract

Calcium is an important second messenger in eukaryotic organisms. Alterations of complex Ca^{2+} homeostatic mechanisms are implicated in a huge variety of disorders, for example cancer, cardiac and neurodegenerative diseases.

A high percentage of *Saccharomyces cerevisiae* genes are highly conserved to mammalian gene sequences, including genes coding for proteins involved in cellular metabolism, autophagy and ageing. Thus, yeast is used as a model organism to explore diverse eukaryotic cellular mechanisms, among them processes involved in longevity.

Autophagy is a cellular degradation process that facilitates the breakdown of proteins and organelles and achieves the rearrangement of cellular components, cell homeostasis and regulates aging. Previous studies have shown a connection between autophagy and life extension.

The Golgi Ca^{2+}-ATPase *PMR1* enables Ca^{2+} transport into the Golgi and the endoplasmic reticulum (ER). The human homolog to *PMR1* is ATP2C1, which upon mutation leads to the skin disorder Hailey-Hailey disease.

It had been published that mutants of *PMR1* show decreased intracellular Ca^{2+} concentrations, changed Ca^{2+} flux and a massive accumulations of Ca^{2+} in vacuoles compared to wild type cells. Thus, calcium homeostasis and autophagy are influenced by Pmr1. That is the reason why my master thesis deals with effects caused by *PMR1* deletion.

We confirmed that cytosolic as well as total Ca^{2+} levels are increased in cells lacking a functional *PMR1* gene. Analysis of transient cytosolic calcium responses indicated that wild type cells could react promptly to high doses of externally supplied Ca^{2+}, whereas this response was slowed down in cells lacking Pmr1. Pre-treatment with Ca^{2+} compensated for the lack of Pmr1, leading to almost similar responses to external Ca^{2+} pulses in wild type and *Δpmr1* cells.

This study demonstrates that *Δpmr1* cells exhibit lower viability compared to wild type cells as well as a deregulation of autophagy. A combination of nitrogen starvation, which is known to induce autophagy, and Ca^{2+} pre-treatment completely rescued *Δpmr1* cells.

Furthermore, we demonstrate that inhibition of the Ca^{2+}/calmodulin-dependent phosphatase calcineurin by the immunosuppressive compound FK506 can restore autophagy defects of cells lacking *PMR1*.

In summary, enhancement of calcium levels and lower viability of *PMR1* deletion mutants were partly prevented by Ca^{2+} pre-treatment. Calcineurin inhibition restored autophagy defects of *Δpmr1* cells.

These data suggest that deletion of *PMR1* results in increased levels of cytosolic calcium. This may induce age-related lethality, excessive activation of calcineurin and down-regulation of autophagy.

Our results might even help to provide new insights into the connection between calcium homeostasis and autophagy. This can be an important fundament for developing of new therapeutic strategies to deal with the Hailey-Hailey disease in future.

Zusammenfassung

Kalzium stellt einen wichtigen sekundären Botenstoff in Eukaryonten dar. Kalziumhomöostase spielt eine bedeutende Rolle in der Aufrechterhaltung zellulärer Funktionen, die bei Abweichungen zu schweren humanen Erkrankungen führen können, z.B. Herzleiden, neurodegenerative Erkrankungen und Krebs.

Das Erbmaterial der Bäckerhefe *Saccharomyces cerevisiae* weist eine hohe Ähnlichkeit zu dem der Säugetiere auf. Dies betrifft auch eukaryotische zelluläre Mechanismen und Prozesse, die Langlebigkeit bewirken. Daher werden viele Studien in *S. cerevisiae* durchgeführt.

Autophagie beschreibt einen Prozess, der zum Abbau von Proteinen und Zellorganellen führt. Dadurch werden Wiederaufbau zellulärer Komponenten, Zellhomöostasis und Alterungsprozesse reguliert, die zu einer Lebensverlängerung führen können.

Die Golgi Ca^{2+}-ATPase *PMR1* ermöglicht den Kalziumtransport in den Golgiapparat und in das endoplasmatische Redikulum (ER). Mutationen im humanen Homolog ATP2C1 können zur dermatologischen Hailey-Hailey Krankheit führen.

Es wurde bereits beschrieben, dass die Deletion von *PMR1* zu einer Erhöhung der zellulären Ca^{2+} Konzentration, einer Veränderung im Ca^{2+}-Fluss und zu einer Anlagerung von Ca^{2+} in der Vakuole führt. Aufgrund von Zusammenhängen zwischen Ca^{2+}-abhängigen Signalübertragungen und Autophagie werden in dieser Masterarbeit Auswirkungen einer *PMR1* Deletion untersucht.

In dieser Arbeit konnte bestätigt werden, dass die Deletion von *PMR1* zu einem erhöhten Ca^{2+} Spiegel in Hefe führt. Sowohl zytosolisches- als auch gesamt-Kalzium ist gegenüber Zellen des Wildtypen (WT) erhöht. Nach externer hoher Kalziumzugabe konnte beobachtet werden, dass in WT Zellen der zytosolische Kalziumwert schnell wieder die Grundhöhe erreicht, wohingegen Zellen mit fehlendem *PMR1* zweimal höhere Kalziumwerte erreichen. Dieser Effekt kann aber durch vorrangegangene Kalziumzugabe aufgehoben werden.

Des Weiteren konnte gezeigt werden, dass sich die Abwesenheit von Pmr1 massiv auf die Lebensfähigkeit auswirkt.

Unter Standardbedingungen ist eine massive Reduktion der Autophagie und eine erhöhte Letalität bei *Δpmr1* Zellen zu beobachten. Eine vollständige Rettung kann durch Kombination von Stickstoffmangel und zusätzlicher Kalziumzugabe erzielt werden.

Wir konnten zeigen, dass durch Inhibierung des Transkriptionsregulators Calcineurin, durch FK506 der Autophagiedefekt aufgehoben werden kann.

Zusammenfassend konnte in dieser Arbeit gezeigt werden, dass das Fehlen von Pmr1 zu einem erhöhten Kalziumspiegel und zu einer Verschlechterung der Lebensfähigkeit führt. Diese Effekte können durch eine frühzeitige Kalziumgabe größtenteils aufgehoben werden. Durch Inhibierung von Calcineurin kann die Aktivierung von Autophagie wiederhergestellt werden.

Diese Daten weisen darauf hin, dass die Deletion von *PMR1* zu erhöhten Kalziumwerten führt. Dadurch können möglicherweise altersbedingte Letalität, gesteigerte Calcineurin-aktivierung und Verminderung von Autophagie verursacht werden.

Unsere Daten könnten helfen neue Erkenntnisse im Zusammenhang zwischen Kalzium und Autophagie zu gewinnen und damit beitragen eine zukünftige Therapiemöglichkeit für Hailey-Hailey Patienten zu finden.

Content

1. Introduction

1.1 Yeast as model organism

The genome of *Saccharomyces cerevisiae* has been completely sequenced in 1996. Yeast harbors 16 chromosomes, with a size of ~12 kilobases[1]. Nowadays *S. cerevisiae* is one of the major model organisms to delineate evolutionary conserved processes in eukaryotes. The reasons are as follows: *S. cerevisiae* is a unicellular eukaryotic organism, it contains membrane-bound organelles, such as a nucleus, endoplasmic reticulum (ER), and mitochondria. Yeast cells divide under optimal laboratory conditions once every 90 min through budding. In nature *S. cerevisiae* cells are able to switch between two mating types: haploid MATa cells mate with haploid MATα cells to form diploids[2]. For this study stable haploid MATa strains were used.

Yeast cells are easy to handle in laboratory work and pose no risk to public health. *S. cerevisiae* cells form colonies on agar plates in 2-3 days. Yeast cells are preserved by freezing at -80°C in a glycerol stock. Either on plasmids or within the yeast chromosomes, genes can be moved in and out. Manipulation or deletion of genes and the study of corresponding phenotypes is easy to achieve in yeast cells[2].

S. cerevisiae possesses highly conserved gene sequences compared to mammalian genes, including genes coding for proteins involved in cellular metabolism, autophagy and ageing. These are reasons why yeast is an optimal model organism to explore eukaryotic cellular mechanism as well as longevity[3].

1.2 Autophagy and ageing

The term *autophagy* is originated from Greek “auto” (self) and “phagy” (eating) and generally describes the cellular catabolic processes in which cytoplasmic components become degraded. The protein machinery necessary for autophagy is extremely conserved in eukaryotic organism. “Self-eating” is necessary for degradation of cytoplasmic materials, as well as for the cytosol, organelles and macromolecules. Important tasks of autophagy are to ensure the recycling of cellular components and cell homeostasis. Altered autophagic levels are linked to a range of human diseases[4,5].

A main regulator of autophagy is the target of rapamycin (TOR). The function of this nutrient-sensing kinase depends on two conserved multiprotein complexes, termed TORC1 and TORC2. TORC1 is a main regulator of cell growth and sensitive to rapamycin. TORC2 participates in actin cytoskeleton forming and also in cell growth. Cellular stress, nitrogen starvation, energy reduction and growth factors regulate the TOR pathway. Under optimal growth conditions, TOR is activated and drives nutrient transport, ribosome biogenesis and initiation of translation. Nitrogen starvation, energy reduction or stress cause an inactivation of the TOR kinase activity which in consequence inhibits cell growth (Figure 1)[6].

TOR is an evolutionarily conserved regulator of growth and metabolism in all eukaryotic cells. Studies using flies, worms, yeast and mice describe an important role for TOR in the regulation of aging[7].

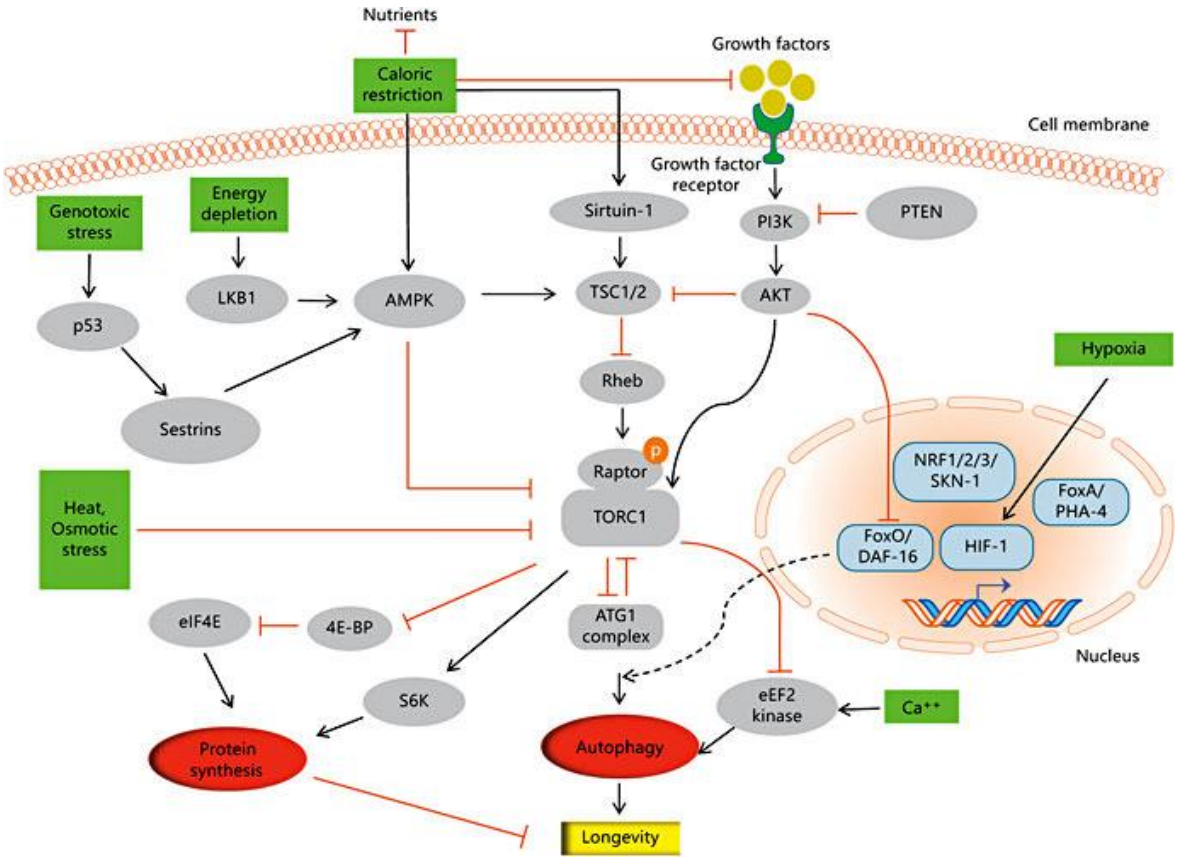

Figure 1: The autophagy pathway and TOR signaling. *The TOR kinase comprises two conserved multiprotein complexes: TORC1 and TORC2. Activity of TORC1 is regulated by nutrients, growth factors, energy levels and stress responses. Under normal growth conditions autophagy is obstructed by inhibition of the Atg1 complex and TOR upregulates translation and stimulates cell growth and metabolic activity. Nitrogen starvation, energy reduction or stress causes in an inactivation of TOR kinase activity which inhibits cell growth. But autophagy is switched on and induces longevity. Black arrows show positive stimulation and red lines indicate an inhibition[6]. Source: adopted from Markaki & Tavernarakis, 2013.*

An important regulator of cell growth and metabolism is mTORC1. It consists of five subunits, including Raptor, which binds ULK1, and mTOR. The Atg1/ULK1 complex is highly conserved in eukaryotic cells, termed Atg1 in yeast and ULK1 in mammals. Low levels of cellular energy activate AMP-activated protein kinase (AMPK), which results in an inhibition of mTORC. Under optimal growth conditions phosphorylation induces inhibition of autophagy initiation. Under starvation conditions, treatment with rapamycin or deletion of TOR, mTORC1 segregates from the ULK1 complex, which results in an upregulation of macroautophagy and longevity[6,8,9].

mTOR is also a conserved checkpoint protein kinase, that adjust cell growth and regulates protein synthesis. Phosphorylation of 4E-BPs and S6Ks are caused by activated mTOR and stimulate anabolic processes through improved translation[10,11].

The activity of the eukaryotic elongation factor 2 (eEF2) kinase is dependent on Ca^{2+} and calmodulin and is controlled by mTOR signaling pathway. Phosphorylation of eEF2 causes in inhibits of protein elongation. Thus, eEF2 represents one of the many links between Ca^{2+} signaling and the mTOR-regulated autophagy[12–14].

In summary, TOR is a key enzyme in the regulation of autophagy. Environmental signals such as limitation of nutrients or energy, exposure to growth factors as well as cellular stress regulate autophagy and increase survival and lifespan in eukaryotic cells. TOR signaling works as a pacemaker of aging and provides an important drug target for age–related diseases and longevity[7].

Three different mechanism of autophagy have been described in humans: Macroautophagy, microautophagy and chaperon mediated autophagy.

Microautophagy is described by an invagination of the lysosomal membrane in connection directly with proteins and organelles, which became sequestered and degraded in the lysosome[15,16].

Chaperone-mediated autophagy (CMA) is an alternative pathway of autophagy. Substrate proteins are carrying a specific peptide sequence (KFERQ). This motif enable proteins to transfer chaperone-dependent from the cytosol to the lysosomal membrane and enter into the lumen for degradation[16–19]. Chaperone-mediated autophagy is caused by nitrogen

starvation as well as oxidative stress[17,18]. Modification in the CMA pathway have been linked with lysosomal disorders, diabetes mellitus and Parkinson's disease [19–21].

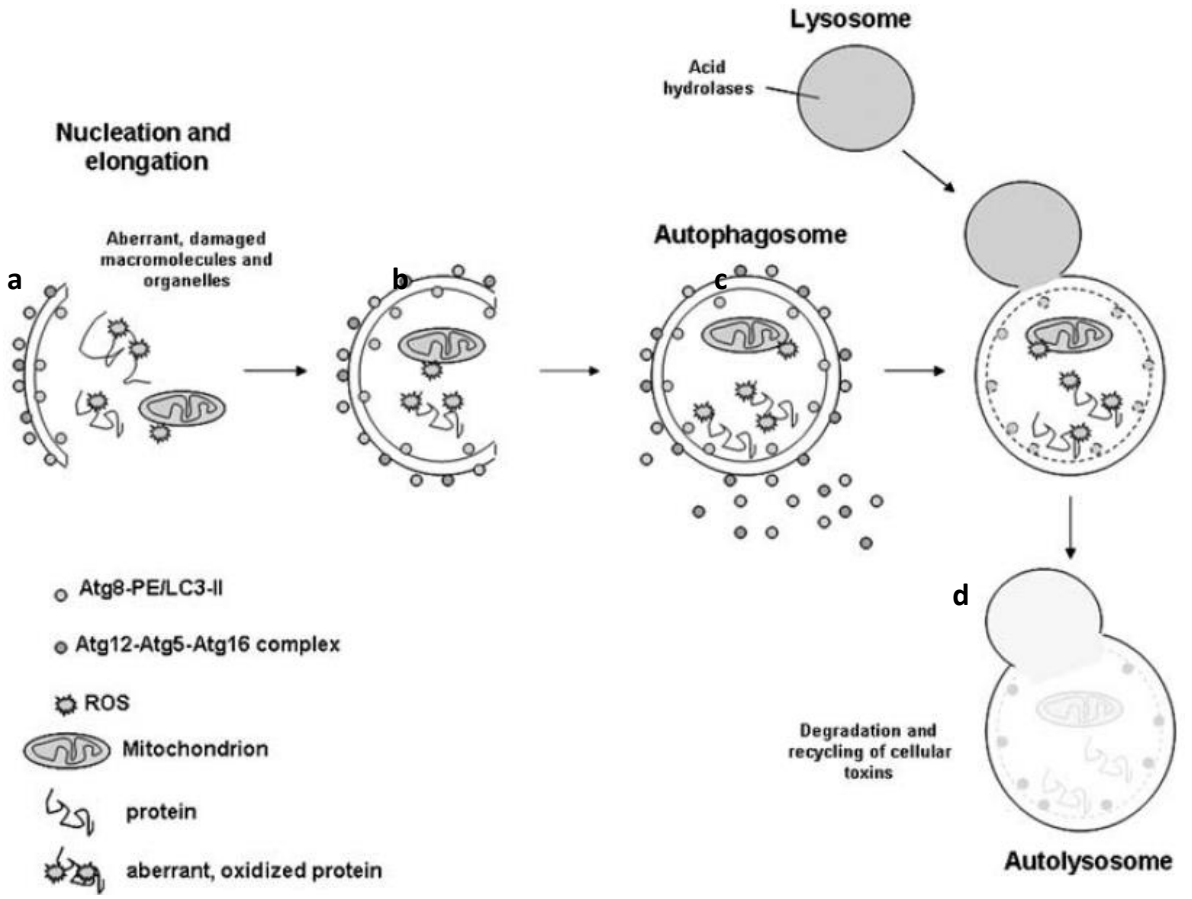

Figure 2: Macroautophagy leads to degradation of altered cellular components. *This mechanism works as follows: (a) Establishment of autophagosomal membrane (depending of Atg8 and the Atg12–Atg5–Atg16 complex), (b) elongation, (c) enclose to an autophagosome, fusion with the lysosome and formation of an (d) autolysosome, where cellular components become degraded by hydrolyses and turn into energy resources and re-usable molecules [22]. Source: adopted from Vellai, 2009.*

Macroautophagy (in this work referred to as "autophagy") is the chief intracellular catabolic instrument for degradation and recycle of long-lasting proteins and organelles. The mechanism of macroautophagy is illustrated in Figure 2. Transmission of an environmental starvation signal activates the autophagosome-generating apparatus. At first the autophagosomal cytosolic double-membrane is established by Atg8 and Atg12–Atg5–Atg16 complex, becomes elongated and engulfs cellular material.

This autophagosome merges with the lysosome to the autolysosome in mammalians and fuses with the vacuole in yeast cells. This lysosome/vacuole contains hydrolytic enzymes to

degrade cellular components and turn it into energy resources and re-usable molecules. Resulting amino acids and lipids are transported to the cytoplasm for recycling[22–24].

In *S. cerevisiae*, about 30 *ATG* (autophagy-related) proteins have been described to be involved in different autophagic processes. Among these, about 17 Atg proteins are essential for the formation of the autophagosome[24].

The localization of Atg8, which is essentially involved in autophagosome formation, changes severely after shift to starvation conditions. During growth, Atg8 stays at tiny dot structures distributed throughout the cytoplasm. During starvation, Atg8 localizes in large punctate structures, the autophagosomes. These autophagosomes are transported to the vacuole, where they are degraded. It has been known for a long time that Atg8 is transcriptionally upregulated in answer to starvation[25].

The autophagy related protein Atg8 is involved in autophagosome formation and is degraded by hydrolytic enzymes in the cytosol (see Figure 2).

During autophagy translation of Atg8 is increased. As Atg8 is a marker for autophagosomes and is targeted to the vacuole during autophagy, its vacuolar degradation represents a mean to quantify the level auf autophagic flux. High levels of Atg8 could result from induced autophagy, but also a disruption in later phases of autophagy could trigger this result. Tagging Atg8 with GFP is a common method to detect Atg8 using microscopy or immunoblotting[26,27].

1.3 Regulation of Ca^{2+} homeostasis and autophagy

Calcium is a general, dynamic and highly conserved second messenger of eukaryotic organisms ranging from yeast to humans. Calcium is necessary for survival, just as for apoptosis and autophagy. In the event of apoptosis, calcium signaling induces cell death. Autophagy has been suggested to be controlled by several calcium depended mechanisms, and these may play an important role in cell survival[28].

It is hardly surprising that intracellular Ca^{2+} signaling regiments autophagy. It has been published that calcium can both act as activator and inhibitor of autophagy depending on

the specific scenario. Ducuypere et al offered a possible declaration: "When cells are healthy and growth conditions are beneficial, small, spontaneous IP_3R-mediated Ca^{2+} signals arise from the ER into the mitochondria for enhancing mitochondrial bioenergetics. Inhibition of this signal leads to activation of autophagy due to the aberrantly low energy production. When cells encounter stress conditions, Ca^{2+} signaling is enhanced and elevated cytosolic Ca^{2+} signals will stimulate autophagic flux. In this way, cells can switch their Ca^{2+} signal from inhibitory to activatory, with respect to autophagy"[29].

In yeast, most of cellular calcium is localized in the vacuole. *S. cerevisiae* shows a total vacuolar Ca^{2+} concentration of ~2 mM (bound to vacuolar polyphosphate) and vacuolar free Ca^{2+} concentration of ~30 µM[30].

The endoplasmic reticulum (ER) plays an important role in protein synthesis and Calcium storage. The concentration of calcium in the ER is highly dynamic and depends on Ca^{2+} uptake by pumps and channel-dependent Ca^{2+} release. Alterations of these complex Calcium homeostatic mechanisms can cause numerous diseases[31–33], for example cardiac hypertrophy, sudden cardiac death[34–36], neuronal diseases like Alzheimer disease and Huntington[37–39] and cancer[40,41]. Referenzen überprüfen

1.4 *PMR1* and *COD1:* Two ATPases involved in cellular Ca^{2+} homeostasis

In 1989 two new genes coding for ATPases have been identified in yeast: *PMR1* and *PMR2*. The sequences showed similarity to other known Ca^{2+} ATPases[42]. After a period of 10 years it had been published, that Pmr1 is a Golgi Ca^{2+}-ATPase pump[43]. Pmr1 also enables Ca^{2+} transport to the endoplasmic reticulum (ER). Deletion mutants of *PMR1* show a decrease of free Ca^{2+} in the ER from 10 to ~5 µM[44] and exhibit higher rates of Ca^{2+} influx compared to its wild type background[45]. Furthermore, deletion of *PMR1* causes increased intracellular Mg^{2+} levels and causes manganese toxicity[46]. It has been demonstrated that *PMR1* deletion led to elevated levels of intracellular Ca^{2+} concentration ($[Ca^{2+}]_i$), in comparison to WT strains. In addition, it was shown that *Δpmr1* cells displayed massive accumulation of Ca^{2+} in the vacuoles and affects the levels of Ca^{2+} flux in yeast cells[47].

It has been published that deletion of *PMR1* inhibits α-synuclein driven increased cytosolic Ca^{2+} levels and cell death, resulting in a prevention of α-synuclein-mediated loss of dopaminergic neurons in a Drosophila model for Parkinson's disease[48]. In addition, it has been shown that Pmr1 is an essential regulator of the target of rapamycin (TOR) and deletion of *PMR1* results in a resistance against rapamycin[49].

The genes *PMR1* (YGL167C: 187616-190468) and *HUR1* (YGL168W: 187464-187796) partly overlap (about 148 bp) (Figure 3) on chromosome VII[50,51]. The DNA sequence of *PMR1* is shown in the attachment. In absence of Hur1, cells are sensitive to hydroxyurea, but the exact function of Hur1 is still unknown[52].

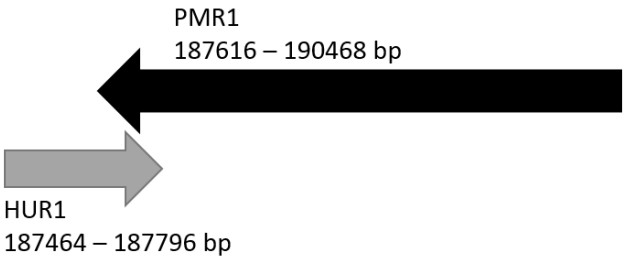

Figure 3: The DNA sequences coding for PMR1 and HUR1 partly overlap.

Cod1 (or Spf1) was characterized as an P-type ATPase in yeast, located in the endoplasmic reticulum (ER) membrane[53,54]. In the absence of Cod1, cellular calcium homeostasis is impaired and transcriptions of calcium-regulated genes are elevated. Double knockout of *PMR1* and *COD1* (*Δpmr1Δcod1)* show increased cellular calcium concentrations[55].

1.4.1 **Hailey-Hailey disease**

The first reference of familial benign chronic pemphigus (or Hailey-Hailey disease) goes back to the Hailey–Hailey brothers in 1939[56]. Hailey–Hailey disease (HHD) indicates an autosomal dominant skin disease. It is described by suprabasal cell separation of the epidermis. In HHD patients the gene *ATP2C1* is mutated. *ATP2C1* encodes a P-type Ca^{2+}-transport ATPase, which is homologous to the Golgi Ca^{2+} pumps *PMR1* in *S. cerevisiae*[57].

Human *ATP2C1* is located to the Golgi apparatus in keratinocytes. It has been reported that Hailey–Hailey disease keratinocytes show increased cytoplasmic Ca^{2+} baseline levels

compared to normal keratinocytes. Actin reorganization is depended of enhanced calcium levels and disturbed in HHD keratinocytes. In addition, Ca^{2+} fill-up is slower in HHD keratinocytes and reaches significantly lower calcium concentrations in the Golgi[58–60].

Intracellular calcium-depended stress seems to be one important aspect of Hailey-Hailey disease, but other facets could not be excluded[61].

Until now, there is no cure for HHD and treatment only reduces the symptoms[62]. Most HHD patients are treated with corticosteroids, antibiotics and antimycotic ointments[63,64]. It has also been reported that Hailey-Hailey disease can be effectively treated with topical tacrolimus (FK506), a known inhibitor of calcineurin[65].

1.4.2 **Calcineurin and FK506 inhibitor**

As already described calcium is an important second messenger of all higher organisms and necessary for survival. Also autophagy is regulated by several calcium-depended mechanisms, and these may be important for longevity[28].

Calcium signaling and transport provides a well-organized network, containing channels, pumps and various Ca^{2+} dependent proteins [31,32] (see Figure 4).

The plasma membrane proteins Mid1 and Cch1 are essential for Ca^{2+} influx in yeast cells[66,67]. Ca^{2+} are transported into the ER by the Golgi pump Pmr1[43,44]. The vacuolar Ca^{2+} ATPase Pmc1 and the Ca^{2+}/H^{+} exchanger Vcx1/Hum1 transport Ca^{2+} into the vacuole[68], where most of cellular calcium is localized[30].

Calcineurin (a Ca^{2+}- and calmodulin-dependent phosphatase) regulates the Crz1 transcription factor in *S. cerevisiae* and requires necessary genes for Ca^{2+}, Mn^{2+}, Na^{+} tolerance and cell wall damage such as *PMR1, PMC1, PMR2A* and *FKS2*[69,70]. Calcineurin is regulated by intracellular calcium levels. During low Ca^{2+} concentrations, calcineurin is incapable to bind calmodulin. During high levels of intracellular Ca^{2+}, Calcium bind to calmodulin and induce a conformational change. Subsequently, the Ca2+/calmodulin complex binds to calcineurin and activates its phosphatase activity[71,72]. It is proposed that calcineurin negatively regulates yeast growth. Pmr1 and Pmc1 impede calcineurin activation by Calium removel of the cytosol and prevent inhibition of growth[73].

Calcineurin is involved in the activation of human T-cell. Calcineurin-calmodulin function is inhibited by the immunosuppressive drug FK506 through development of a drug-dependent complex. The complex FKBP-FK506 competitively binds to calcineurin and inhibits its functions[74,75].

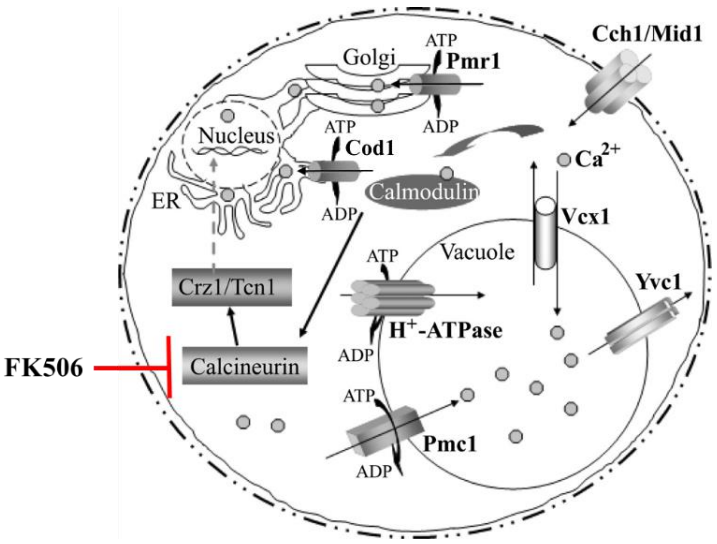

Figure 4: Calcium signaling and transport in S. cerevisiae. *Ca^{2+} were transferred into the cytosol by the plasma membrane channel complex Cch1/Mid1. Cytosolic Ca^{2+} and calmodulin activated calcineurin. Calcineurin enables activation of the transcription factor Crz1/Tcn1 and target genes become transcribed. Ca^{2+} is transported by ATPases into the Golgi (Pmr1), ER (Cod1) and vacuole (Pmc1) or by the vacuolar H^+/Ca^{2+} exchanger Vcx1[76]. FK506 competitively binds to calcineurin and inhibits its function[74]. Source: Ton and Rao, 2004.*

FK506 (Tacrolimus), a novel immunosuppressor was isolated from *Streptomyces tsukubaensis* and described in 1987[77]. Tacrolimus is used to prevent graft rejection in organ transplantation patients[78].

Publications indicate that Hailey-Hailey disease can be effectively treated with FK506[65].

1.5 Aim of work

The role of calcium as second messenger is extremely conserved[28]. Alterations in the molecular mechanisms governing Ca^{2+} homeostasis are implicated in numerous diseases[31], for example cardiac hypertrophy as well as sudden cardiac death[34–36], neurodegenerative diseases like Alzheimer disease and Huntington[37–39] and cancer[40,41].

Intracellular Ca^{2+} signaling can stimulate or inhibit autophagy[29]. Autophagy is necessary for degradation of cytoplasmic materials, as well as for cytosol, macromolecular complexes and organelles.

PMR1 encodes for the main Golgi Ca^{2+}-ATPase in *S. cerevisiae* and enables Ca^{2+} transport to the Golgi and ER[43,44]. Previous studies showed that *PMR1* deletion causes elevated $[Ca^{2+}]_i$ levels and changed Ca^{2+} flux[47]

The aim of this work was to establish Pmr1 as molecular link between calcium homeostasis and autophagy.

The important questions of this work were:

Is deletion of *HUR1* influencing *PMR1* deletion mutants?

Does deletion of *PMR1* influence autophagy and survival?

How do *PMR1* deletion mutants respond to rapamycin treatment?

Can external Ca^{2+} restore the defects of *PMR1* deleted cells?

2. Methods and materials

2.1 Microbiological methods

Growth media

All growing media were prepared using deionized water and sterilized by autoclaving (121°C for at least 20 min). For agar plates, 2% agarose was added bevor autoclaving.

For synthetic media a 10x stock solution of amino acid mixtures, were autoclaved separately and stored at -20°C. Also a 10x stock solution of YNB+AS (Yeast nitrogen base and ammoniumsulfat) was prepared and autoclaved separately and stored at room temperature (RT). Stock solutions of amino acid mixtures (10x) and YNB+AS (10x) were added to autoclaved media to an one fold endconcentration and stored at room temperature (compare with material section)

Growth media with Ca^{2+}, rapamycin and FK506 pre-treatment

Overnight cultures (ONC) were always prepared in SMD media without any treatments. Main cultures were inoculated to an OD_{600} 0,06 in 7-10 ml SMD.

$CaCl_2$ (10 mM) and rapamycin (40 nM) were added to main culture immediately.

For FK506 treatment (0,5 µM) cells were inoculated in 10 ml SMD, corresponding an OD_{600} 0,08 instead of OD_{600} 0,06. FK506 (0,5 µM) was also added immediately to main cultures.

Liquid cultures

Bacterial strains were inoculated in LB media (37°C, 145 rpm).To *E.coli* strains, which contained plasmids, ampicillin was added to the media (endconcentration: 100 µg/ml) to select for the plasmid.

Saccharomyces cerevisiae (*S. c*.) strains without plasmids were grown in YPD medium or synthetic media containing all amino acids (SMD) at 28°C with shaking at 145 rpm.

S. c. strains containing plasmids were grown in synthetic media, lacking the amino acid corresponding to the selections marker on plasmids (e.g. –his, -leu).

Plate cultures

E. coli was grown on LB plates for one day at 37°C, adding 100 µg/ml ampicillin if necessary. *S. cerevisiae* was streaked out on solid media in petri plates. Different media were used, depending on contained vectors, compared to liquid cultures. Plates were incubated for two days at 28°C and stored at 4°C.

Plasmid isolation from *E. coli*

Cell cultures of 2 ml ONC were harvested and supernatant was removed. The pellet was resuspended in 100 µl solution I (4°C). Then 200 µl solution II were added, mixed carefully and incubated on ice for 5 min. The solution became clear and viscous. 150 µl of Solution III was added and the cell suspension was centrifuged for 10 min (full speed, 4°C). Supernatant was removes and the pellet was incubated with 800 µl ethanol (absolute, RT) for 5 min, centrifuged for 10 min (4°C). The pellet was washed with ethanol (80%, 4°C) and centrifuged for 10 min.

Supernatant was removed and the tube was dried at 37%, afterwards the pellet was resuspended in 30 µl ddH_2O and stored at -20°C.

E. coli transformation

A volume of 40 µl of competent *E. coli* cells and 1 µl of DNA were mixed carefully in a sterile reaction tube and incubated on ice. Solution was transferred to a sterile electroporation cuvettes (UV radiation), electroparated and resuspended with 1 ml LB media and incubated for 30 min at 37°C. Cells were harvested and 100 µl of cell suspension were plated on LB plates (100 µg/ml ampicillin) and incubated at 37°C overnight.

Yeast transformation for plasmids

An overnight culture (ONC) was prepared in YPD. A volume of 15 ml YPD were inoculated to an approximate OD_{600} of 0,1 and were incubated 4-6 hours (145 rpm, 28°C). Cells were harvested (3500g, 3 min) washed in 10 ml ddH_2O resuspended in 10 ml 0,5x TE /1x LiAc. Pellet was resuspended in 300 µl 1x TE /1x LiAc and incubated for 30 min at 28°C.

Competent yeast cells (50 µl), vector DNA (1-5 µg) and carrier DNA (5 µl, salmon sperm DNA, denaturated at 95°C, 10 min) were mixed in a sterile reaction tube with adding 300 µl 1x TE / 0,5x LiAc / 40% PEG and incubated at 28°C for 30 minutes. Afterwards the cells were heat shocked at 42°C for 20 min. Cells were harvested by centrifugation, washed and resuspended in 100 µl aqua bidest. The cell suspension was plated onto selective SMD agar plated, lacking the amino acid corresponding to the selections marker on plasmids (e.g. –his, -leu). The plates were incubated at 28°C for two days. Colonies were selected and streaked out on fresh selective plates and afterwards stored.

Generation of competent yeast cells

Cells were inoculated in 25 ml YPD media (OD_{600}=0,2) and grew to an OD_{600} 0,5-0,7. Cells were harvested by centrifugation and washed once with 0,5 volume ddH_2O and one with 0,25 volume SORB. The suspension was centrifuged and pellet was mixed with 180 µl SORB and 20µl carrier DNA on ice, aliquoted to volumes of 50 µl and stored at -80°C.

Yeast transformation for linear DNA

Competent cells (50 µl) and ~7µl DNA were mixed with 342 µl PEG and incubated for 30 min (inverting mixture every 10 min). A volume of 42 µl DMSO (final concentration of 10%) was added and heated at 42°C for 15 min. Cells were harvested (3 min, 2000 rpm). The pellet was resuspended in 50-100 µl YPD and plated onto YPD plates.

Storage

Strains were grown in in YPD or selective media overnight, mixed with the same volume of 50% glycerol and stored at -80°C.

Deletion of *PMR1*: knock-out cassette

The knock out cassette for deletion of *PMR1* was prepared with following primers. Deletions were carried out in *S. cerevisiae* BY4741 strain.

sense
CAGCACAGACGTAAGCTTAAGTGTAAGTAAAAGATAAGATAATCAGCTGAAGCTTCGTACGC

antisense *(Δpmr1Δhur1c^{148})*:
ATGTGACATATCAAACATTTGAGAAATACGTTGAGTCTTCTTCGCATAGGCCACTAGTGGATCTG

antisense *(Δpmr1*)

TAACAGAGACAGTCCAACGGCGTAGTTGAACATTTTGTTGCATAGGCCACTAGTGGATCTG

PCR reaction: Taq-polymerase (0,5 µl), dNTPs (5 µl), Thermopol Buffer (5 µl), forward primer (0,5 µl), reverse primer (0,5 µl), ddH_2O (38 µl).

PCR program:1: 5 min 95°C; 2: 25x: 1 min 95°C, 1 min 58°C, 2 min 72°C; 3: 10 min 72°C

pYM-PCR for ATG8 endogen GFP tagging

PCR reaction mixed on ice: Template (pYM-ATG8; 1 µl (=100 µg/ml), dNTPs (2 mM; 8,75 µl), Buffer 2 (10x; 5 µl), S1 primer (1:10; 3,2 µl), S4 primer (1:10; 3,2 µl), ddH_2O (18,35 µl). Q5-polymerase (0,5 µl).

PCR program: 1:3-4 min 97°C; 2: Hot start cycles: 1 min 97°C, 30 sec 54°C, 2 min 40 sec 68°C; 3: 20 cycles: 1 min 97°C, 30 sec 54°C, 2 min 40 sec 68°C +20s/cycle.

S1 Primer:

5´- CTAATAATTGTAAAGTTGAGAAAATCATAATAAAAATAATTACTAGAGACATGCGTACGCTGCAGGTCGAC-3´

S4 Primer:

5'-GACTCCGCCTTCCTTTTTTCAAATGGATATTCAGACTTAAATGTAGACTTCATCGATGAATTCTCTGTCG-3´ [79,80]

A fraction (2 µl) of PCR product was analyzed by agarose gel electrophoresis. The remainding sample was EtOH precipitated. An equal amount of sample volume of ammonium acetat (5 M) was added. Twice the amount of EtOH (abs.) was added at incubated at room temperature for 30 min and centrifuged by high speed for 15 min. Ice cold EtOH (70%) was added to the pellet, decanted carefully and air dried. DNA can used for linear yeast transformation.

Clonogeniticy plate assay

Overnight cultures (ONC) were prepared in SMD media. For main culture an OD_{600} 0,06 was inoculated in 10 ml SMD. At desired time points serial 1:100 and 1:10.000 dilutions of culture in ddH_2O were prepared. Cells were countered with CASY Cell counter, used a 1:10.000 dilution. The exact volume containing 500 cells were plated onto YPD agar plates and incubates on 28°C for two days. Cell colonies were countered by Colony counter (Lemna Tec) and colony forming unites (CFU) were determined.

Clonogenic survival assay

Overnight cultures (ONC) were prepared in SMD media. For main culture an OD_{600} 0,06 was inoculated in 7-10 ml SMD or SMG. If a shift schema is used, cells grew in 50 ml SMD for six hours. Cells were harvested and washed with ddH_2O two times. A main culture cells were inoculated to OD_{600} 0,8 in 7-10 ml nitrogen starvation media. $CaCl_2$, Rapamycin and FK506 were added to main culture immediately, ONC was prepared in standard SMD media.

For chronological ageing 30-200 µl of cells were stained with PI and/or DHE at indicated time points. A number of 3000 cells were determined by flow cytometry and positive and negative populations were quantified by FACSDiva software.

Fluorescent microscopy

Autophagy induction was observed by cellular localized GFP-Atg8. Cells were stained with popidium iodid (PI) as described. GFP fluorescent signal was detected using an eGFP filter and for PI fluorescent signal a dsRED filter was used.

2.2 Biochemical methods

Chemical lysis

A volume corresponding to 2,5 units of OD_{600} were harvested (1 min, 13.000 rpm), supernatant removed, stored at -20°C or lysed immediately. For lysis, the pellet was resuspended in lysis buffer (200 µl) and incubated on ice for 10 min. Suspension was mixed with TCA (55%, 200 µl) and incubated on ice for 10 min. After centrifugation (10 min, 13.000 g, 4°C) the supernatant was removed completely and the pellet was resuspended in urea loading buffer (150 µl). The samples were heated at 65°C for 10 min and Tris solution was added if necessary. Samples have been used for SDS-Polyarcylamide gel electrophoresis immediately or stored at -20°C.

SDS - Polyarcylamide gel electrophoresis

A volume of 10-15 µl of cell extracts from chemical lysis were loaded on stacking gel. Electrophoresis was performed in Tris-Glycin-SDS buffer at a current of 12 mA per gel. Page Ruler (2 µl) Prestained protein ladder was utilized.

Immunoblotting

Proteins were transferred to PVDF membrane using the tank-blot-system with transfer buffer for 60 min at 220 mA.

To avoid unspecific bindings, the membranes were incubated in milk powder dissolved in TBS solution (3%) for one hour. After washing with 1x TBS-T the membrane was incubated with primary antibody overnight at 4°C or 1h at room temperature. After washing with 1x TBS-T (3 times) the membrane was incubated with secondary antibody for 1 hour.

Detection was performed using the ECL system. After incubation the fluorescent signal was detected by ChemiDoc (BIO-RAD) or using X-ray films and quantified by software (Bio-Rad).

ATG8-GFP based autophagy assay

S. cerevisiae clones with an endogenously GFP-tagged ATG8 gene was used to perform autophagy assays as well as microscopic images.

DHE- and PI-staining

An ONC is always prepared in SMD Media. For analysis PI or DHE positive population, cells were inoculated in 7-10 ml SMD or SMG to OD_{600} 0,06. For shift schemata cells were grown 6 h in SMD (50-100ml), harvested by centrifugation, washed with ddH_20 two times and inoculated in nitrogen starvation media to OD_{600} 0,8 (7-10 ml).

At selected time points, 30-200 µl of culture were transferred into a 96 well microtiter plate and centrifuged for 10 min at 4.000 rpm. Supernatant was removed and cells were resuspended in 250 µl of an 1:1.000 dilution of DHE (2,5mg/ml stock) or in 250 µl of an 1:1.000 dilution of PI (100µg/ml stock) in 1x PBS. The plate was incubated for 10 min in the dark, centrifuged and resuspended with 250 µl 1x PBS. Samples could be used for FACS analysis as well as for microscopy.

Flow cytometric determination of propidium iodide (PI) uptake is a method for observing cell death. Intact membrane of viable cells excludes the propidium ion. Loss of this permeability barrier results in PI staining. But studies has shown that cells are able to repair membrane damages[81].

DHE staining is used to evaluate the impact of oxidative stress. When DHE is presented in cells, ROS will oxidize dihydroethidium (DHE) to fluorescent ethidium that can be detect by a flow cytometer[82].

Aequorin Luminescence measurement of cytosolic calcium levels

Cytosolic Calcium $[Ca^{2+}]_{cyt}$ levels were measured using yeast strains carrying the vector pYX212 (selectionmarker –Leu) encoding the bioluminescent protein aequorin under the control of a TPI promotor. For analysis of resting, basal $[Ca^{2+}]_{cyt}$ and for cellular response to high dose of external Ca^{2+}, cells were inoculated in SMD (-Leu) to OD_{600} 0,06. For shift schemata cells were grown 6h in SMD-Leu, harvested by centrifugation, washed with ddH20 two times and inoculated in nitrogen starvation media to OD_{600} 0,8.

At indicated time points, an equivalent of 6*10^6 cells (determined by Casy cell counter) were harvested into a 96 well plate. The pellets were resuspended in 200 µl media (the same as for growing) containing 4 µM coelenterazine and incubated for 1 h in the dark. To remove excess coelenterazine cells were harvested and resuspended in 200 µl media for further 30

min. The basal luminescence was measured per well in 0,5 sec intervals for 25 sec. In order to investigate the kinetics of the cellular response to an external Ca^{2+} shock, a pump injected 40 µl of a 0,9 M $CaCl_2$ solution into each well (endconcentration: 150 mM $CaCl_2$), meanwhile the signal for kinetic limunescence measurements was recorded for 70 sec. The signals were normalized to OD_{600} of each well.

Measurement of total calcium levels by Calcium Detection Kit (abcam, ab102505)

For analysis of total calcium levels cells were inoculated in SMD to OD_{600} 0,06. At indicated time points 3 OD_{600} unites were harvested, washed with 500 µl ddH_2O very quickly, stored at -20°C or instantly processed. Pellets were resuspended with 40 µl 1 M HCl and cooked at 99°C for 20 min. Cell suspension was neutralized by 40 µl NaOH (1 M) and centrifuged with 13.000 rpm for 5 min. 10 µl of supernatant was transferred in a 96 well plate and diluted with 20 µl ddH_2O. For the standard curve, calcium concentrations ranging 1,5 to 0,023 mM were prepared. For total calcium measurement 30 µl of assay reaction mixture was added in each well and the fluorescence intensity was recorded with a fluorescence plate reader at Ex/Em =540/590 nm.

2.3 Materials

Buffers and solutions

If not mentioned separately, all media, buffers and solutions, were prepared using ddH_2O. All pH-values are adjusted at room temperature.

Saccharomyces cerevisiae growth media

Media	**Contents**
YPD (full media)	1% Yeast Extract (BD Biosciences) 2% Bacto Peptone (BD Biosciences) 4% Glucose (AppliChem)
Minimal synthetic media (SMD / SMG)	0,17% Yeast Nitogen Base (BD Bioscience) 0,5% Ammonium sulfate (ROTH) 2% Carbon source D: Glucose (AppliChem) G: Galactose Amino acids: 80 mg/l histidine 200 mg/l leucine 30 mg/l all other amino acids Nucleotides: 30 mg/l adenine 30 mg/l uracil
Caloric restriction media (SMD containg 0,5% Glucose)	0,17% Yeast Nitogen Base (BD Bioscience) 0,5% Ammonium sulfate (ROTH) 0,5% Carbon source D: Glucose (AppliChem) Amino acids: 80 mg/l histidine 200 mg/l leucine 30 mg/l all other amino acids Nucleotides: 30 mg/l adenine 30 mg/l uracil

Nitrogen starvation media (SD-N / SG-N)	0,17% Yeast Nitrogen Base (BD Bioscience) 2 % Carbon source D: Glucose (AppliChem) G: Galactose
YPD / SMD / SMG Agar	As indicated above, adding 2% Agar-Agar
Rapamycin	Stock: 1 mg/ml in DMSO
$CaCl_2$	Stock: 1 M $CaCl_2$ in ddH_2O
FK506	Stock: 2,5 mM in DMSO

Plasmid isolation from E. coli

Solution	**Contents**
Solution I	50 mM Glucose, 10 mM EDTA, 25 mM Tris-HCl; pH 7,5
Solution II	0,2 M NaOH, 1% (w/v) SDS
Solution III – 3M Potassium acetate	5 M Potassium acetate (60 ml), Acetic acid (11,5 ml) in ddH_2O (18,5 ml); pH 4,8

Yeast Transformation

Vector DNA

Solution	**Contents**
10 x TE	100 mM Tris in ddH_2O; pH 7,5; 10 mM EDTA
10x LiOAc	1 M Lithium acetate in ddH_2O
50% PEG	50% Polyethlene glycol (3350) in ddH_2O
Carrier DNA	Salmon sperm DNA (10 mg/ml); denatured at 95°C for 10 min, put on ice for 10 min

Linear DNA

Solution	**Contents**
SORB	100 mM LiOAc, 10 mM Tris/HCl pH 8,1; 1M EDTA/NaOH pH 8,1, 1M sorbitol
10x LiOAc	1 M Lithium acetate in ddH_2O

PEG	100 mM LiOAc, 20 mM Tris/HCl pH 8,1; 1 M EDTA/NaOH pH 8, 40% Polyethlene glycol (3350) in ddH_2O
DMSO	Dimethyl sulfoxide
Carrier DNA	Salmon sperm DNA (10 mg/ml); denatured at 99°C for 10 min, put on ice for 10 min

pYM-PCR for ATG8 endogen GFP tagging

Solution	**Contents**
10x Buffer 2	500 mM Tris/HCl pH 9,2; 22,5 mM $MgCl_2$, 160 mM NH_4SO_4, 20% DMSO, 1% Triton-X100

Solutions for measurement cell number (CASY Cell counter)

Solution	**Contents**
Casyton	0,9 mM NaCl, 0,1 mM EDTA
Casyclean	Contents are not specified

Used antibodies

Antibody	**Dilutions**
Primary antibodies:	
α-GFP	1:5.000 in TBS + 1% milk powder
α-GAPDH	1:40.000 in TBS + 1% milk powder
Secondary antibodies:	
HRP- α-mouse	1:10.000 in TBS + 1% milk powder
HRP- α-rabbit	1:10.000 in TBS + 1% milk powder

Solutions for SDS PAGE and Western Blot analysis

Solution	Contents
Stacking gel	250 mM Tris / HCl ph 6,8 0,2% SDS 5% acrylamide 0,13% N.N´-methylen-bisacrylamide 0,1% ammonium peroxidesulfate (APS) 0,01% N.N.N´N´-tetramethylethylenediamine
Seperating gel (12,5%)	250 mM Tris / HCl pH 6,8 0,2% SDS 12,5% acrylamide 0,4% N.N´-methylen-bisacrylamide 0,1% ammonium peroxidesulfate (APS) 0,01% N.N.N´N´-tetramethylethylenediamine
Electrophoresis buffer (Tris-Glycine)	25 mM Tris / HCl 192 mM glycine 0,2% sodium dodecyl sulfate (SDS) pH 8,8
Standard	PageRuler prestained protein ladder
Urea Loading Dye	200 mM Tris / HCl 8M urea 5% SDS 1 mM EDTA 0,02% Brominephenolblue 15 mM DTT, pH 6,8
Blotting Buffer (CAPS)	10 mM Caps 10% methanol in ddH_2O; pH 11
TBS TBS-T	50 mM Tris / HCl pH 7,6, 150 mM NaCl Adding 0,02% Triton
Blocking solution	1% milk powder in TBS
<u>ECL reagents</u> Clarity Western ECL Substrate ECL western blotting detection reagent	 Bio Rad, USA GE Healthcare-Amersham

DNA electrophoresis

Solution	Contents
Agarose	Company:PEQLAB
1x TAE	80 mM Tris / acetic acid pH 8,0 0,2 M EDTA
Ethidium bromide 6x sample loading buffer	Company: Fermentas

DHE and PI staining

Solution	Contents
1x PBS	25 mM potassium phosphate buffer pH 7,0 0,9% (w/v) NaCl
DHE (dihydroethidium)	Stock: 2,5 mg/ml in Dimethylsulfoxide 1:1000 diluted in PBS
PI (propidium iodide)	Stock: 100 µg/ml 1:1000 diluted in PBS

Cytosolic Calcium measurement via Aequorin

Solution	Contents
Coelenterazine h	Stock: 40 µM in ethanol (abs.), Life Technologies
0,9 M $CaCl_2$	Stock: 2 M $CaCl_2$ Diluted in ddH_2O

Measurement of total calcium levels by Calcium Detection Kit

Product name	Company
Calcium Detection Kit (Colorimetric) (ab102505)	abcam

2.4 Equipment

Equipment	Company
Centrifuges	
6415R	Eppendorf, Germany
3-18K	Sigma, UK
3-18KS	Sigma, UK
5415R	Eppendorf, Germany
Z400K	Hermle, Germany
Z216 MK	Hermle, Germany
Spectrophotometer	
DU730	Beckman coulter
Thermomixer	
ThermoSTat plus	Eppendorf, Germany
Thermomixer Compact	Eppendorf, Germany
Cell counter CASY	Schaerfe System, Germany
Colony counter	Lemna Tec
Flow cytometer	
BD LSR FortessaTM Cell Analyzer	BD Biosciences, USA
Wett electroblotting apparatus	
Mighty small transphor	Amersham Biosciences
Transfer membrane	
PVDF (0,45µm)	Carl Roth GmbH + Co, Germany
Power supply	Bio-Rad, USA
Electrophoreseboard for proteine gels	Bio-Rad, USA
Lab Shaker	Infors AG, Swiss
Fluorescence microscope	Zeiss, Germany
Horizontal agarosegelelectrophorese board	
Mini-Sub Cell ST	Bio-Rad, USA
Tecan Genios Pro	Tecan, Austria
Incubation Shakers	
Infors HT Multitron Pro	Infors AG, Swiss
Incubator	Hareaeus, Germany

PCR machines Veriti (96 well thermal cycler) GeneAmp PCR System 9700	 Applied Biosystems Applied Biosystems
Mini-Beadbeater	Biospec Products, USA
ChemiDoc™	Bio-Rad, USA
Luminometer GloMax-Multi Detection system	 Promega

2.5 Strains

All experiments were carried out in Saccharomyces cerevisiae strain BY4741 (MATa, *his3Δ1, leu2Δ0, met15Δ0, ura3Δ0*). Also deletion mutants of *PMR1* and *COD1* were carried out in BY4741.

Yeast strain	**origin**	**Contents**
BY4741 (WT)	MATa his3Δ-1 leu2Δ-0 met15Δ-0 ura3Δ-0	Euroscarf
WT EGFP-ATG8	BY4741 ATG8Δ::natNT2-pATG8-EGFP	
Δpmr1	BY4741 pmr1Δ::kanMX	This study
Δpmr1Δhur1^{c148}	BY4741 pmr1Δhur1^{c148}Δ::kanMX	This study
Δpmr1 EGFP-ATG8	BY4741 pmr1Δ::kanMX::natNT2-pATG8-EGFP	This study
Δcod1	BY4741 cod1Δ::kanMX	Euroscarf
Δcod1 EGFP-ATG8	BY4741 cod1Δ::kanMX::natNT2-pATG8-EGFP	This study

To measure cytosolic Ca^{2+} levels, strains were transformed with pYX212 vector encoding cytosolic aequorin (pYX212-cytAEQ) (kind gift from E. Marteggani, Department of Biotechnology and Biosences, University of Milano-Bicocca, Milan, Italy)[48].

3. Results

3.1 Deletion of *HUR1*^{c148} doesn't effect *PMR1* deletion mutants toxicity

As mentioned in the introduction, the DNA sequences coding for the Golgi Ca^{2+}-ATPase *PMR1* and *HUR1* partly overlap (Figure 3)[43,50,51]. In the BY4741 background strain, two different *PMR1* deletion mutants were generated. In one strain, the whole *PMR1* gene sequence was deleted *(Δpmr1Δhur1*^{c148}), thus *HUR1* was also affected. In the other strain *PMR1* was only partially deleted to leave *HUR1* still intact (in this work referred to as *Δpmr1*). *PMR1* sequence and the primers used for respective deletions are shown in the attachments.

Cells of both *Δpmr1* variants and the WT (BY4741) background strain were aged in liquid culture. At indicated time points cells were stained with PI (propidium iodide) and positive stained cells were quantified by flow cytometry over a period of 21 days. Frequency of cell death (determined by PI pos. cells) indicate that in absence of Pmr1, yeast cells showed a higher mortality rate compared to WT cells.

Both *PMR1* deletion variants exhibited the same cell death rate (Figure 5). Therefore, unless otherwise stated, the following experiments were carried out in *PMR1* deletion strains possessing an intact *HUR1* gene (referred to „*Δpmr1*").

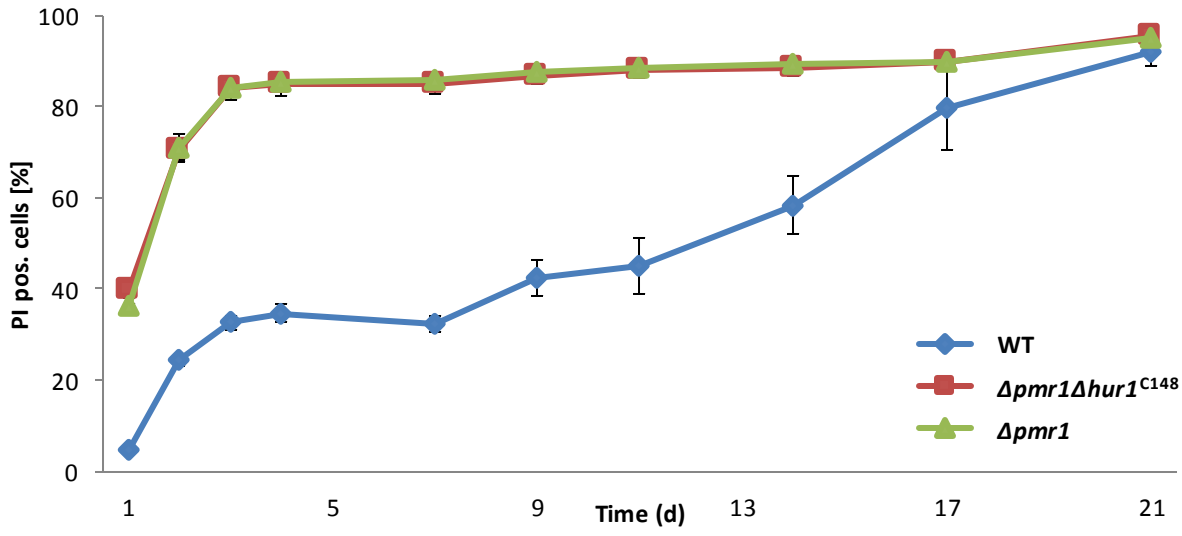

Figure 5: Deletion of PMR1 causes early death during aging. *Viability of WT yeast cells, PMR1 deletion mutants with HUR1 is intact (Δpmr1) and HUR1 is partially mutated (Δpmr1Δhur1* ^{c148}*). Over a period of 21 days, cell death were determined by staining cells with PI (propidium iodide) and analyzed by flow cytometry. n=4*

3.2 *PMR1* deletion mutants exhibit lower viability

We next asked if there is a connection between growth media and toxicity of *Δpmr1* cells. For this reason, viability of *PMR1* knockouts were compared to wild type cells incubated in growth media containing either glucose (SMD) or galactose (SMG) as carbon source. In addition, cells were tested for their response to nitrogen starvation during aging, a regime that is known to (i) induce autophagy and to (ii) require autophagy for survival.

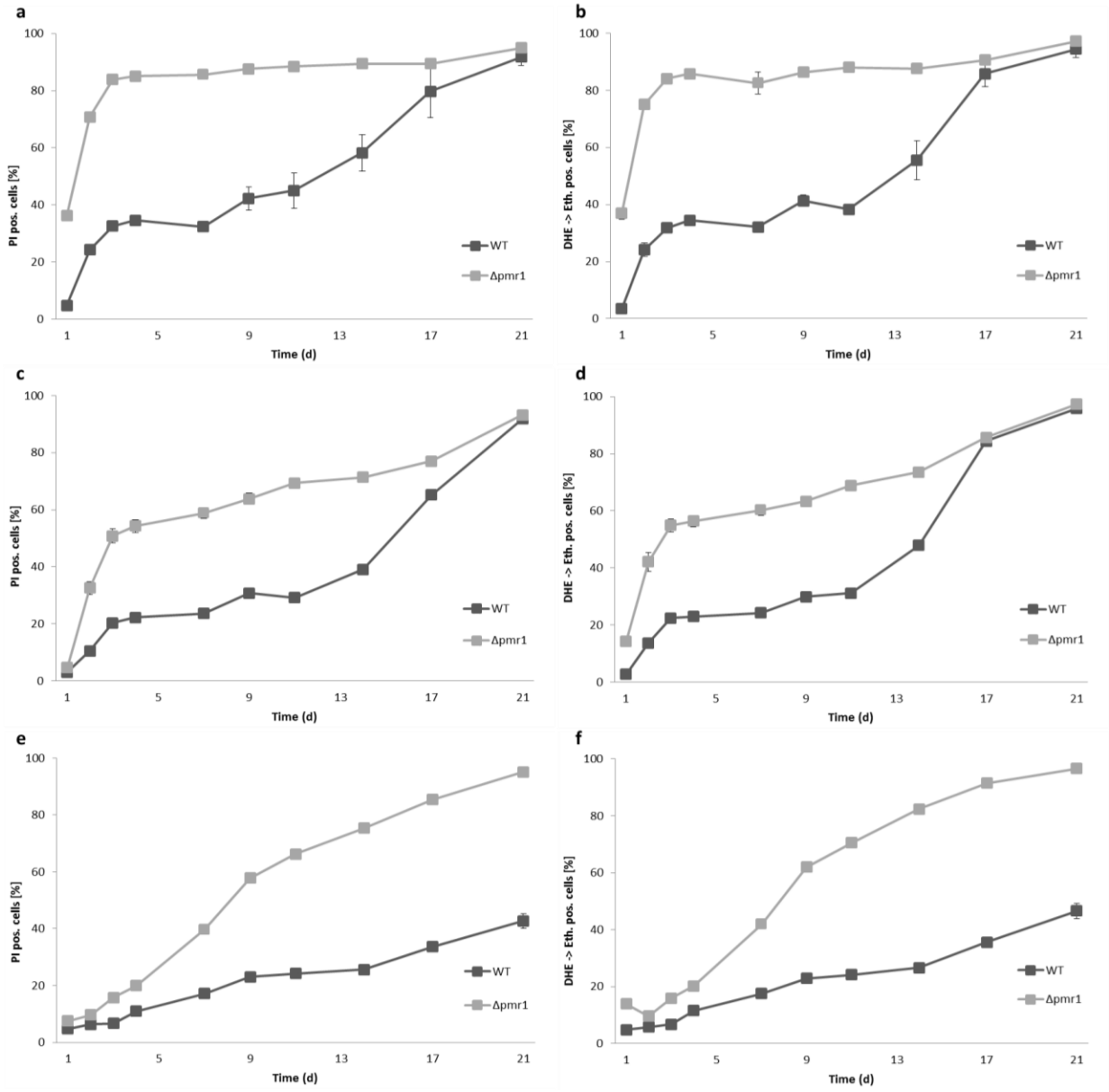

Figure 6: High levels of oxidative stress and cell death is caused by deletion of PMR1. Effect is partly restored by nitrogen starvation. *Flow cytometric quantification of oxidative stress and plasma membrane integrity of WT and Δpmr1 yeast cells. Cells were aged in liquid culture consisting glucose (SMD), galactose (SMG) or any nitrogen sources (SD-N) over a period of 21 days. Age-associated cell death was detected by PI pos. population in cultures inoculated in (a) SMD, (c) SMG (d) and nitrogen starvation media. Quantification of oxidative stress by flow cytometry was displayed by turnover of non-fluorescent dihydroethidium (DHE) to fluorescent ethidium (Eth). WT and Δpmr1 yeast cells were grown on (b) SMD, (d) SMG (f) and nitrogen starvation medium. n=4*

Flow cytometric quantifications were performed over a period of 21 days. At indicated time points of chronological ageing the amount of oxidative stress (specified by transformation of non-fluorescent dihydroethidium (DHE) to fluorescent ethidium (Eth)) and the percentage of dead cells (measured by PI pos. population in culture) were determined by FACS analysis.

Data indicates that both ROS production (DHE staining) and membrane rupture (PI staining) were increased in cells lacking Pmr1 under all conditions (Figure 6a-f).

It could be demonstrated that the composition of the media largely influenced the rate of cell death. In particular, the use of galactose instead of glucose decreased age-related cell death in *Δpmr1* cells.

As published previously, wild type cells were rescued under nitrogen starvation. Also toxicity of *Δpmr1* cells was decreased under nitrogen starvation conditions compared to standard minimal media (SMD), in particular during the first days of the aging.

ROS production compared to plasma membrane integrity leads to the conclusion that the majority of DHE positive cells are almost dead.

It has been demonstrated that age-related cell death depends on media composition. High amounts of lethality were determined by *PMR1* deletions strains grown in minimal medium containing glucose.

Nitrogen starvation conditions can partly restore the lethality of *Δpmr1* cells at early days.

3.3 Increased Ca^{2+} levels in *Δpmr1* cells

As described in the introduction, cells lacking Pmr1 exhibit increased Ca^{2+} levels[55]. Also in the human homolog of *PMR1*, *ATP2C1* mutations lead to increased cytoplasmic Ca^{2+} baseline levels in Hailey–Hailey disease keratinocytes compared with normal keratinocytes[58,59]. To compare *Δpmr1* with another Ca^{2+} ATPase, a deletion of *COD1* (P-type ATPase, located in the ER membrane[53,54]) was also created.

We measured basal cytosolic Ca^{2+} levels in WT, *Δpmr1* and *Δcod1* cells incubated on SMD media for 24h. To this end, we used an aequorin-luminescence-based assay. After binding of Ca^{2+} the photoprotein aequorin produces blue light. Luminescence emission was detected by luminometer and Ca^{2+} values were determined[83].

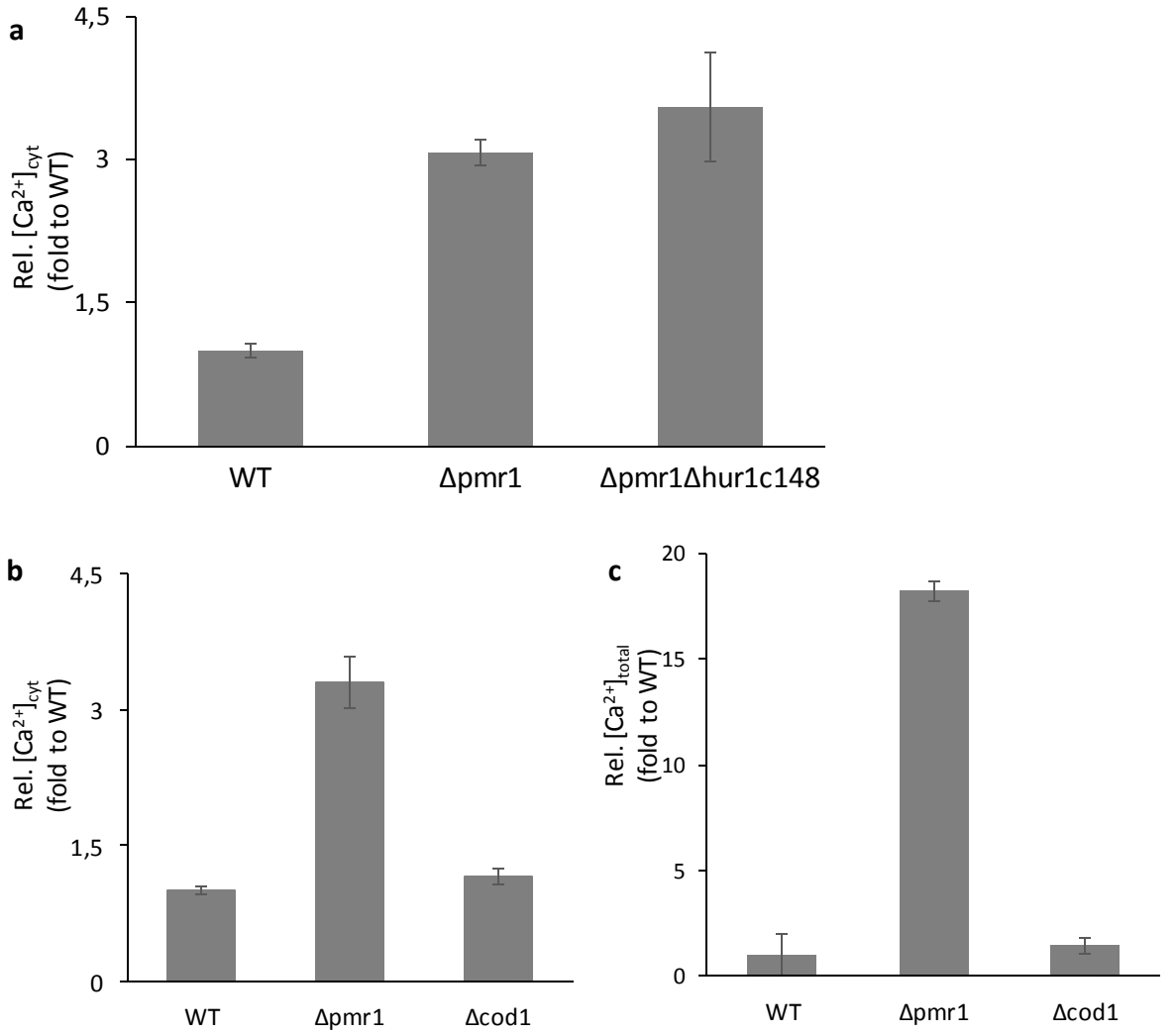

Figure 7: Cytosolic and total Ca^{2+} levels are increased in PMR1 deletion cells. *Aequorin-luminescence-based determination of basal cytosolic Ca^{2+} levels after 24h in culture of (a) Δpmr1, Δpmr1Δhur1^{c148}* and *WT cells n=4-8. (b) WT, Δpmr1 and Δcod1 cells. (n=8) and (c) measurement of total Ca^{2+} levels by Calcium Detection Kit in WT, Δpmr1 and Δcod1 cells inoculated in SMD media for 24 h. n=1-4*

The measurements were performed with in both *PMR1* deletion mutants (*Δpmr1 Δhur1*^{c148} strain and *Δpmr1* strain). Both strains of *PMR1* deletion mutants show almost same calcium levels (Figure 7a). While there is no significant difference in cytosolic Ca^{2+} levels between wild type and *Δcod1* cells, we observed a 3-fold increase in cells lacking Pmr1 (Figure 7b).

Total calcium levels were determined by using "Colorimetric Calcium Detection Kit". BY4741 (WT), *Δpmr1* and *Δcod1* cells were inoculated on SMD for 24h before Ca^{2+} levels were measured (Figure 7c). In the absence of Pmr1, cells show higher total calcium concentrations compared to WT and *COD1* knockout cells.

These two independent measurements indicate that the lack of *PMR1* results in increased cytosolic as well as total intracellular Ca^{2+} levels.

3.4 Lacking of Pmr1 results in downregulated autophagy

To test whether deletion of Pmr1 interferes with autophagic processes, we quantified the levels of autophagy using Atg8-GFP liberation-assays. Strains harbouring an endogenously GFP-tagged Atg8 expressed under its natural promoter were used (see Figure 2). During autophagy Atg8 is targeted to the vacuole and subjected to autophagic degradation. Thus, cleavage of GFP-Atg8 to free GFP was detected by immunoblot analysis using specific antibodies against GFP (green fluorescent protein) and against glyceraldehyd-3-phosphate dehydrogenase (GAPDH) as loading control[27].

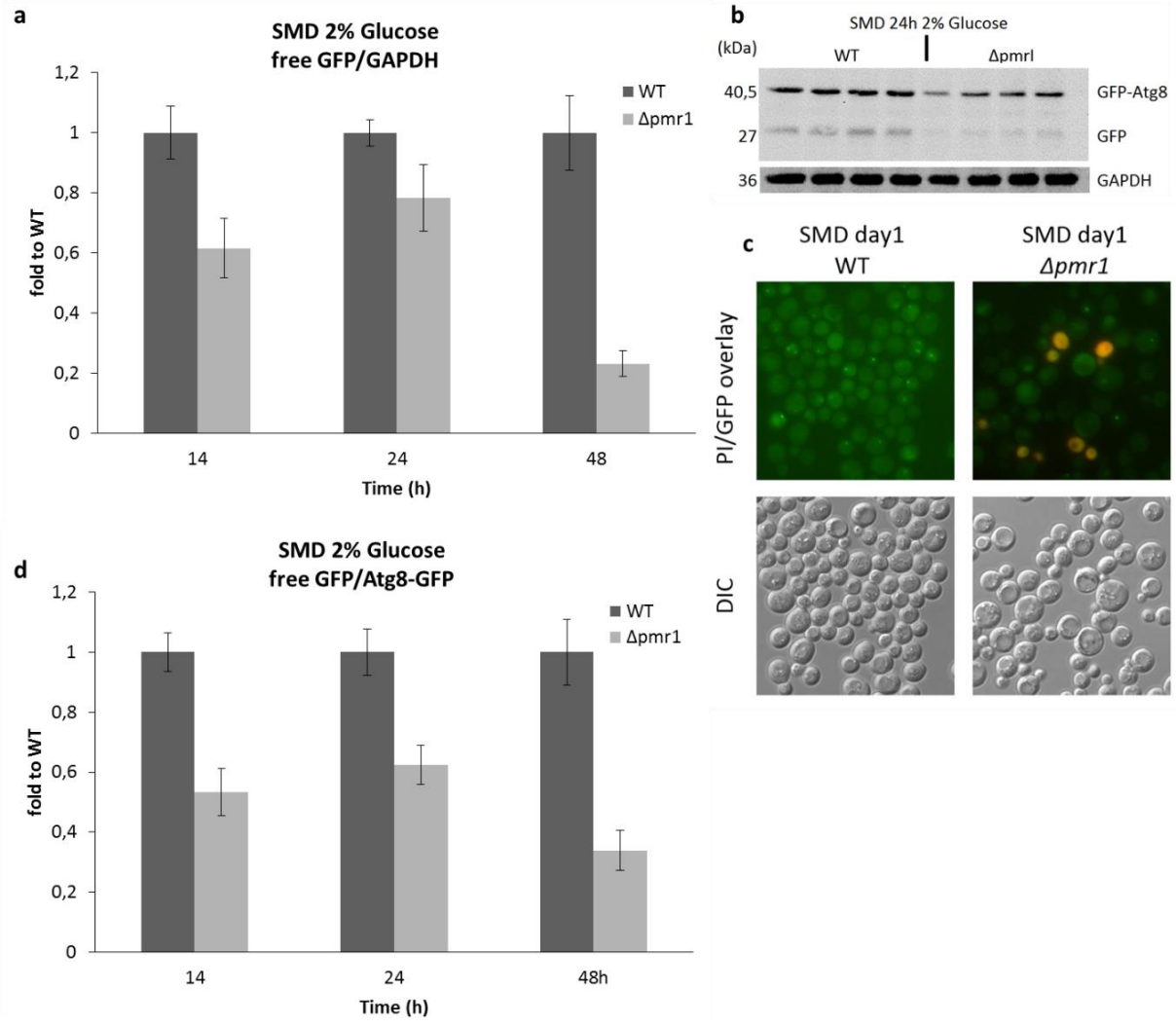

Figure 8: Deletion of PMR1 results in a downregulation of autophagy. *WT and Δpmr1 cells were grown in standard minimal media containing 2% glucose (SMD). For determination of autophagy levels blots were immunodecorated with antibodies directly against GFP (green fluorescent protein) and against glyceraldehyd-3-phosphate dehydrogenase (GAPDH) as loading control. (b) Representative immunoblot analysis and (c) representative fluorescent microscopy of GPF-tagged Atg8 WT and Δpmr1 cells after one day in culture (SMD). (a) Autophagic flux determination by GFP-liberation assay using specific antibody against GFP and GAPDH (loading control) at indicated time points. Ratio of (b) free GFP/GAPDH and (d) free GFP/Atg8-GFP of WT and Δpmr1 were evaluated. n=7-8*

At indicated time points samples of WT and *Δpmr1* yeast cells expressing Atg8-GFP, grown in SMD media containing 2% glucose, were harvested, digested by chemical lysis, separated by electrophoreses, transferred to a membrane and immunodecorated with specific antibodies against GFP and against GAPDH as loading control.

As described in the introduction, Atg8 is a necessary protein in autophagosome formation and is degraded in the vacuole[27]. Representative micrographs of membrane integrity (PI pos.) and GFP (as well as GFP-Atg8) to identify GFP localization as well as a representative immunoblot are depicted (Figure 8a-c).

In order to be able to distinguish between mere changes in the expression levels of Atg8-GFP and disturbances of the autophagic flux, normalized free GFP levels (free-GFP/GAPDH) as well as the vacuolar protein turnover (free-GFP/Atg8-GFP) was quantified (Figure 8a,d).

PMR1 deletion mutants display decreased levels of Atg8 expression and of autophagic flux. Lower ratio in free-GFP/GAPDH indicates a reduced expression level of Atg8, while the turnover of Atg8-GFP protein is quantified by the ratio of free-GFP to Atg8-GFP.

The representative micrographs shown in Figure 8c allow the visualization of Atg8-GFP positive dot-like structures, the autophagosomes. The formation of autophagosomes seemed to be reduced in *Δpmr1* cells compared to wild type cells.

These data suggest lacking of Pmr1, leads to a downregulation of autophagy and a lower autophagic flux compared to its wild type background.

Next, I tested whether nutrient starvation might still be capable of stimulation autophagy in *PMR1* mutants.

3.5 Nitrogen starvation can (partly) restore the autophagy-defect of *Δpmr1* cells

Cells lacking a functional *PMR1* gene show less autophagy compared to wild type cells upon growth on standard minimal media (SMD, containing 2% glucose) (see Figure 8). Nitrogen starvation media doesn't contain any nitrogen resources or amino acids. It results in elevated autophagy levels and cell cycle arrest in G1/G0 phase[84].

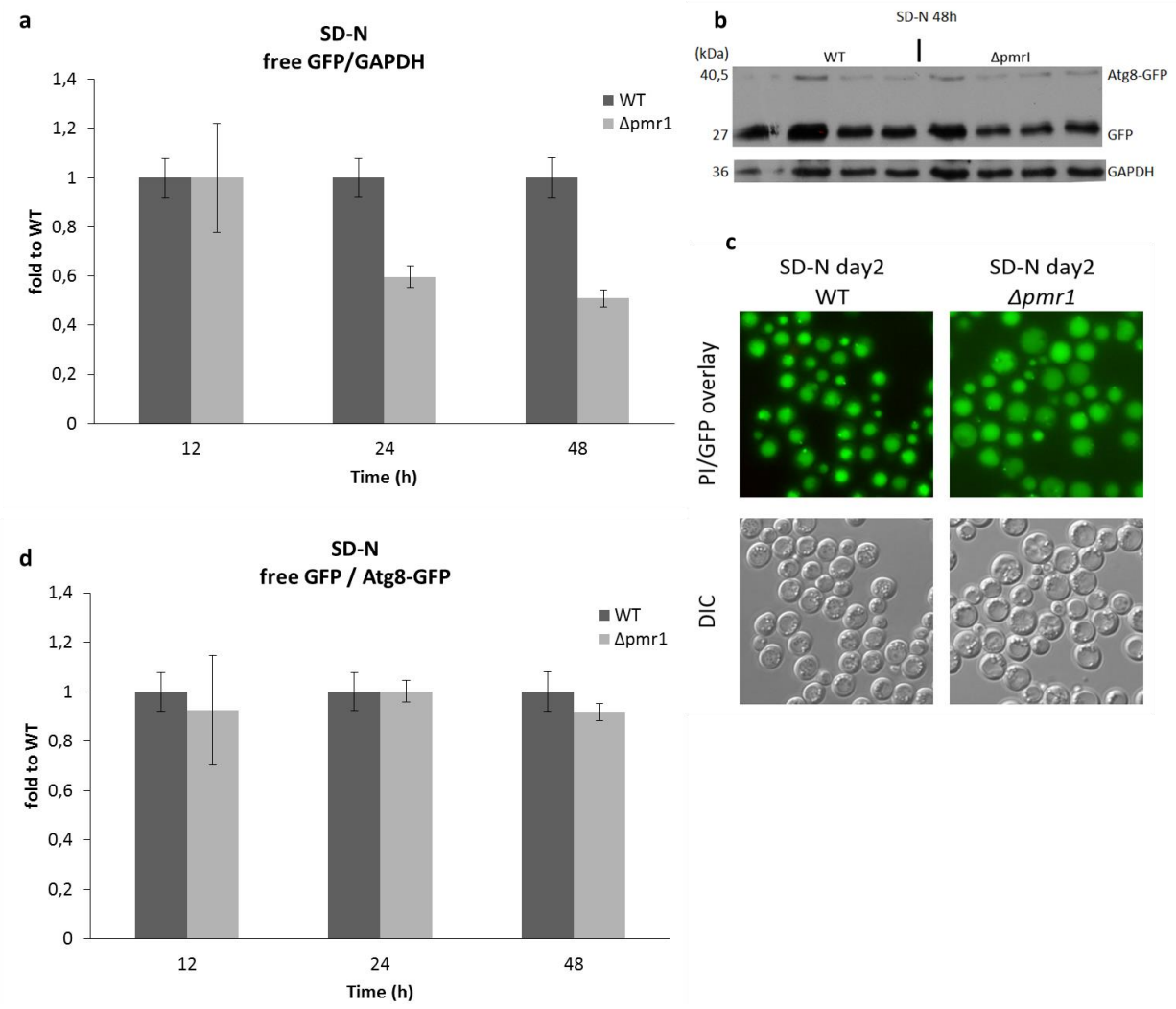

Figure 9: Autophagy defect of Δpmr1 cells is partly restored by nitrogen starvation (SD-N). *WT and Δpmr1 cells were grown 6 h on SMD and then shifted on nitrogen starvation conditions (SD-N). Time specifications are corresponding the sum in liquid cultures (SMD + SD-N). (b) Representative immunoblot analysis of WT and Δpmr1 cells after 48h in liquid cultures. (c) Representative micrographs of PI stained and GFP-tagged Atg8 on the second day. Autophagy levels were determined by liberation of GFP-Atg8. Blots were inoculated by specific GFP- and GAPDH-antibodies (loading control) at specified time points. Autophagy levels of WT and Δpmr1 cells were quantified by (a) free GFP/GAPDH and (d) free GFP/Atg8-GFP signal rates. n=2-24*

Atg8-GFP-liberation assays show that deletion of *PMR1* does only slightly impair autophagic processes under nitrogen starvation. The ratio between free GFP/Atg8-GFP is comparable in cells deleted in *PMR1* and WT cells. So in both strains the same level of Atg8-GFP was degraded in the vacuole.

The ratio between free GFP/GAPDH shows that *Δpmr1* cells express the same levels of Atg8-GFP after 12 h under nitrogen starvation. After a longer period of incubation *PMR1* deletion mutants generate less Atg8-GFP compared to the WT strain (Figure 9a-d).

The micrographs serve to provide evidence of GFP localization in cells and identification of cells with lacking plasma membrane. Pictures also indicated a massive induction of autophagy in WT and *Δpmr1* cell compared to micrographs of SMD inoculated cells (see Figure 8c).

In summary, induction of autophagy is influenced by functional Pmr1. Lacking of *PMR1* inhibits autophagy induction. These effect could be partly restored by nitrogen starvation.

This led to the question if increased autophagy by nitrogen starvation could influence lethality of *PMR1* deletion mutants?

3.6 Nitrogen starvation media reduces *PMR1* deletion induced toxicity

It is shown in Figure 5 that cells lacking a functional *PMR1* gene exhibit lower viability. In addition, *Δpmr1* cells displayed reduced autophagy compared to wild type cells upon growth on glucose (Figure 8). However, as shown in Figure 9, *Δpmr1* cells were not completely autophagy deficient, as they exhibited the same levels of autophagic degradation upon nitrogen starvation as wild type cells.

This led to the question if induction of autophagy by nitrogen starvation influences the toxicity of *PMR1* deletion mutants?

Viability of *PMR1* deletion mutants compared to its WT background inoculated in nitrogen starvation conditions are shown in Figure 10. Cell death was detected by flow cytometric quantification of plasma membrane integrity (valued by PI positive cells).

Nitrogen starvation conditions (SD-N) prolonged the life span of both WT as well as *Δpmr1* cells compared to standard minimal media (SMD). Whilst a rescue of wild type cells could be observed until 21 days, lower toxicity of *Δpmr1* cells was particularly noticeable at early days and disappeared at later time points.

It appears that induction of autophagy by nitrogen starvation partly rescue *Δpmr1* cells lethality.

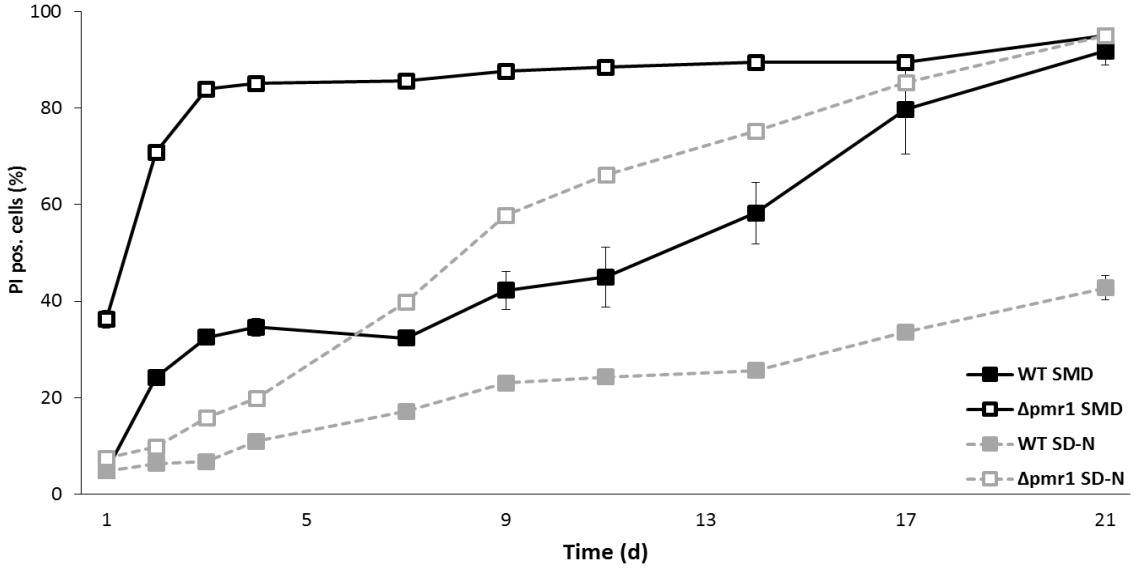

Figure 10: Autophagy defect of Δpmr1 cells is partly restored by nitrogen starvation *Comparison of flow cytometric quantification of cell death (valued by PI-positive cells) of WT and Δpmr1 cells grown in standard minimal media (SMD) and nitrogen starvation conditions (SD-N).*

3.7 Pre-treatment of *Δpmr1* cells with Ca^{2+} decreased calcium levels

As shown in Figure 7, basal cytosolic and total Ca^{2+} levels are increased in *PMR1* deletion mutants compared to WT and *Δcod1* yeast cells. Same experiment was performed with addition of 10 mM $CaCl_2$ immediately to growth media. Cells were grown in two different culture media for 24 h: standard minimal media (SMD) and SMD with extra 10 mM $CaCl_2$. Basal cytosolic Ca^{2+} and total Ca^{2+} levels of WT, *Δpmr1* and *Δcod1* were compared in cells with or without calcium pre-treatment.

Basal cytosolic Ca^{2+} levels were measured with an aequorin-luminescence-based determination. Measurement of total calcium levels were performed using a "Colorimetric Calcium Detection Kit".

Calcium pre-treatment leads to a significant decrease of basal cytosolic Ca^{2+} as well as of total Ca^{2+} levels in *Δpmr1* compared to its wild type background strain (Figure 11).

These results suggest that the calcium pre-treatment has a positive impact on the Ca^{2+} levels of *Δpmr1* cells.

Next, I tested whether Ca^{2+} pre-treatment also effected the fast cellular response to high external Ca^{2+} pulses or ageing.

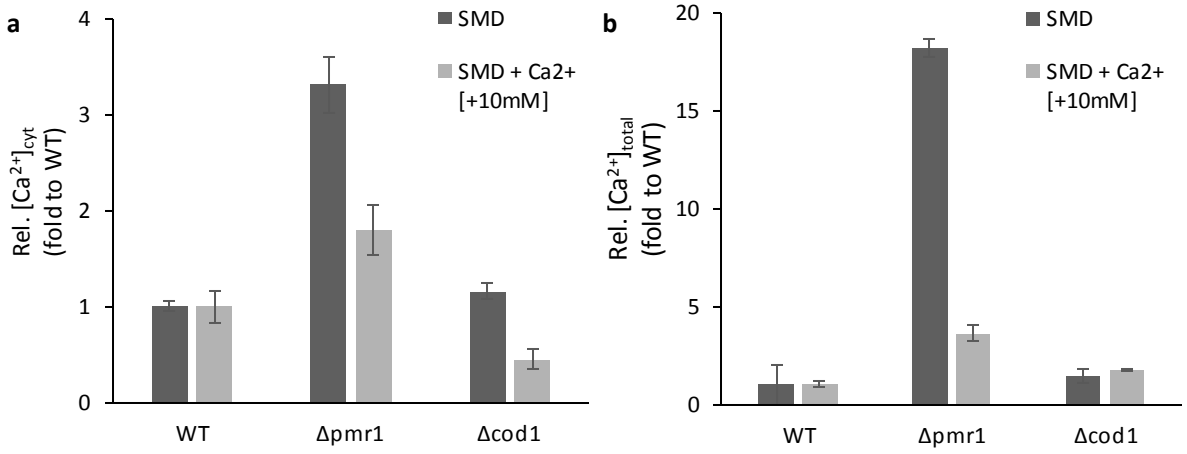

Figure 11: Ca^{2+} pre-treatment decreases basal cytosolic Ca^{2+} as well as total Ca^{2+} level in cells lacking PMR1. *WT, Δpmr1 and Δcod1 cells were inoculated in standard SMD media compared with SMD media treated with 10 mM $CaCl_2$ and were grown for 24h (a) Aequorin-luminescence-based determination of basal cytosolic Ca^{2+} n=4-8 (b) Measurement of total Ca^{2+} levels by Calcium Detection Kit. n=1-4*

3.8 Calcium pre-treatment induced lower $[Ca^{2+}]_{cyt}$ levels

As shown in Figure 11, basal cytosolic and total Ca^{2+} levels are increased in *PMR1* deletion mutants compared to wild type and *Δcod1* yeast cells, inoculated in standard minimal media (SMD) for 24h.

Cytosolic calcium levels were monitored over prolonged periods, using aequorin-luminescence-based determination.

Transient $[Ca^{2+}]_{cyt}$ responses of WT, *Δpmr1* and *Δcod1* cells upon treatment with 150 mM $CaCl_2$ is shown in Figure 12. Deletion of Ca^{2+} ATPases caused a two-times increase of $[Ca^{2+}]_{cyt}$ compared to WT levels. All strains achieve almost same cytosolic Ca^{2+} levels after a period of 25 seconds.

Addition of 10 mM $CaCl_2$ to growth media increased basal Ca^{2+} levels in WT cells. In contrast level of $[Ca^{2+}]_{cyt}$ are deceased in *Δpmr1* cells.

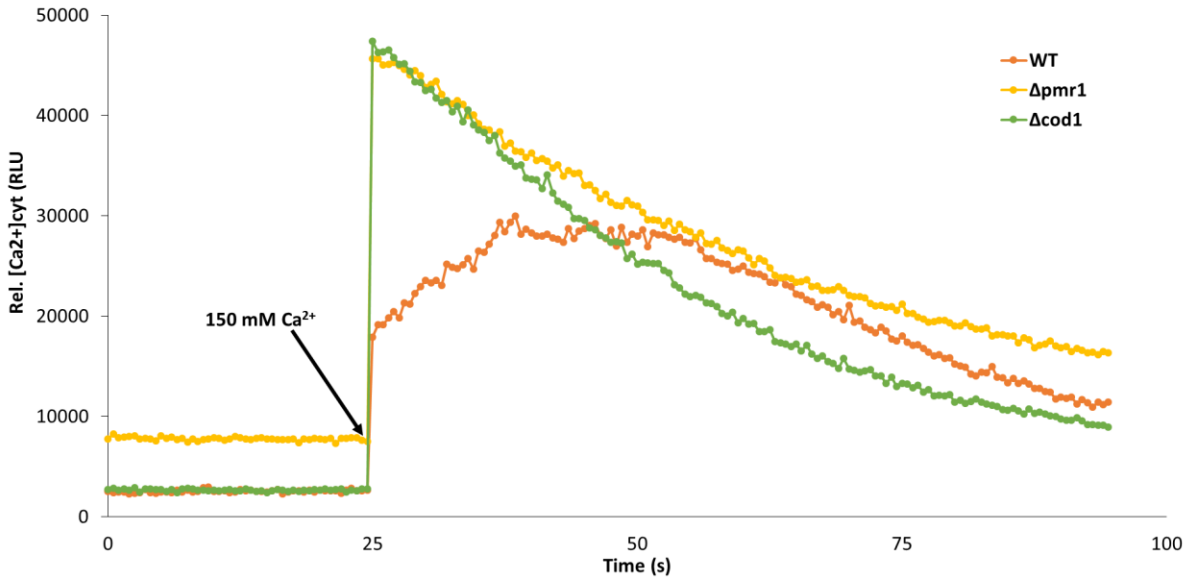

Figure 12: Cells lacking PMR1 or COD1 reach higher cytosolic Ca^{2+} levels than WT cells. *Aequorin-equipped WT, Δpmr1 and Δcod1 cells inoculated into standard minimal media (SMD) for 24 h SMD. After challenged with 150 mM $CaCl_2$ transient $[Ca^{2+}]_{cyt}$ responses were monitored. n=3-4*

After basal Ca^{2+} measurement, cells were challenged with 150 mM $CaCl_2$ and transient $[Ca^{2+}]_{cyt}$ responses were monitored (Figure 13). Calcium untreated cells, lacking a functional *PMR1* gene, responded after challenging with 150 mM $CaCl_2$ with higher cytosolic calcium

levels than WT cell. After 25 sec wild type and *Δpmr1* cells display the same cytosolic Ca^{2+} levels.

Calcium pre-treated *Δpmr1* cells showed an improved calcium response compared to untreated cells, and reach almost wild type levels. It might be that pre-treatment with Ca^{2+} (10 mM) in growth media for 24 h leads to a desensitization to following high calcium concentrations.

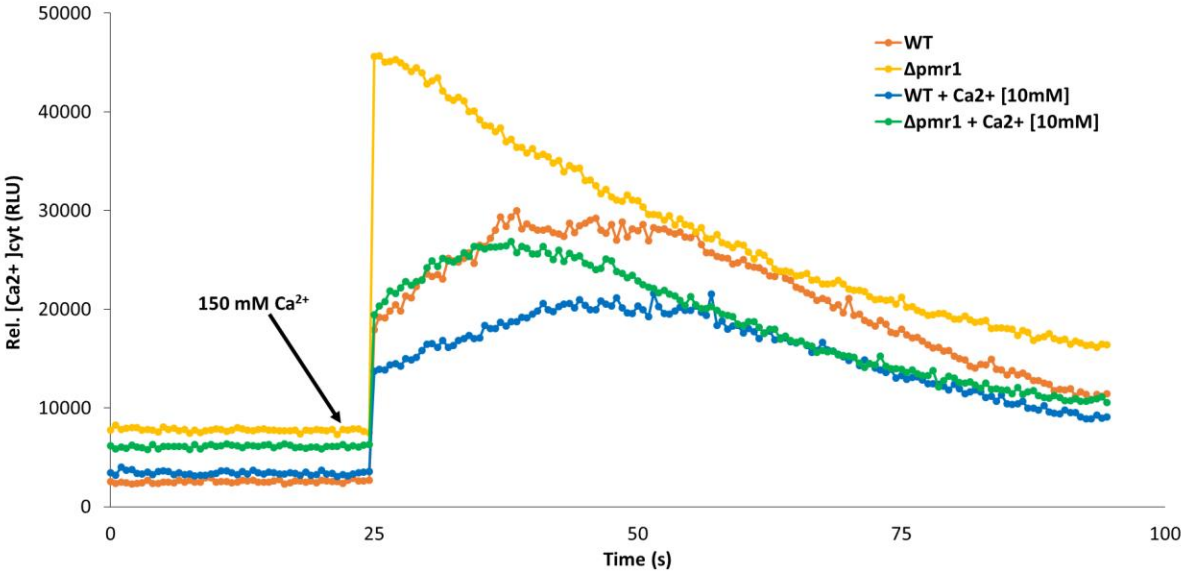

Figure 13: Ca^{2+} pre-treatment improves $[Ca^{2+}]_{cyt}$ responses of cells lacking PMR1. *WT and Δpmr1 cells were inoculated into two different types of culture medium for 24 h: Standard minimal media (SMD) and SMD added 10 mM $CaCl_2$. Cells are challenged with 150 mM $CaCl_2$ and transient $[Ca^{2+}]_{cyt}$ responses were monitored. n=3-4*

The results demonstrate that *PMR1* deletion mutants show an altered cytosolic Ca^{2+} profile as response to high external Ca^{2+} pulses. Calcium pre-treated *Δpmr1* cells showed on the contrary an improved calcium response, resembling almost wild type levels.

An explanation might be that *PMR1* deletion mutants are not able to successfully transport the calcium ions outside the cytosol.

Thus the question arises: Does pre-treatment with Ca^{2+} also positively influence toxicity of *PMR1* deletion mutants?

3.9 Rapamycin and calcium pre-treatment effect lethality

We have seen so far, that lacking of a functional *PMR1* gene causes lower viability. But this strain is not deficient to perform autophagy. Pre-treatment of cells with Ca^{2+} decreases cytosolic calcium levels in *Δpmr1* cells. We also know that nitrogen starvation media induces autophagy - also in case of *PMR1* deletion (Figure 10).

It had been published, that rapamycin treatment results in an upregulation of autophagy and effects longevity[6,8,9].

Chronological ageings of *Δpmr1* and *Δcod1* cells compared to its BY4741 (WT) background strain were performed. Cells were inoculated in different media (Figure 14a-f): (a,b) standard minimal media containing 2% glucose (SMD), (c,d) minimal media containing 0,5% glucose (=caloric restriction) and (e,f) medium containing no nitrogen resources (SD-N). In addition to these media, cells were also incubated in these media containing calcium (10 mM) and rapamycin (40 nM). In summary, nine different growth conditions were compared. Flow cytometric quantification was performed to detect dead cell (as indicated by PI pos. cells) in each mentioned condition at indicated time points.

Results show that *PRM1* deletion mutants exhibited improved viability upon growth in SMD (2% glucose) containing Ca^{2+} in early days. Under these conditions WT and *Δcod1* cells were not positively influenced (Figure 14a).

Rapamycin, an inducer of autophagy, reduced toxicity in each strain on the first and second days. On the last day of ageing (day 6), *PMR1* deletion mutants displayed no difference in cell death compared to rapamycin treated cells (Figure 14b).

Caloric restriction (SMD media containing 0,5% glucose) did not affect age-related cell death of *Δpmr1* cell. Treatment of cells with rapamycin (40 nM) clearly improved the viability of *Δpmr1* cells on day two. But this effect was disappeared at day six (Figure 14c-d).

It is shown in Figure 10 that caloric restriction can partly restore lethal phenotype of *Δpmr1* cells but also increased viability of WT cells. Nitrogen-less media added calcium as well as rapamycin did not obviously influence viability in tested strains.

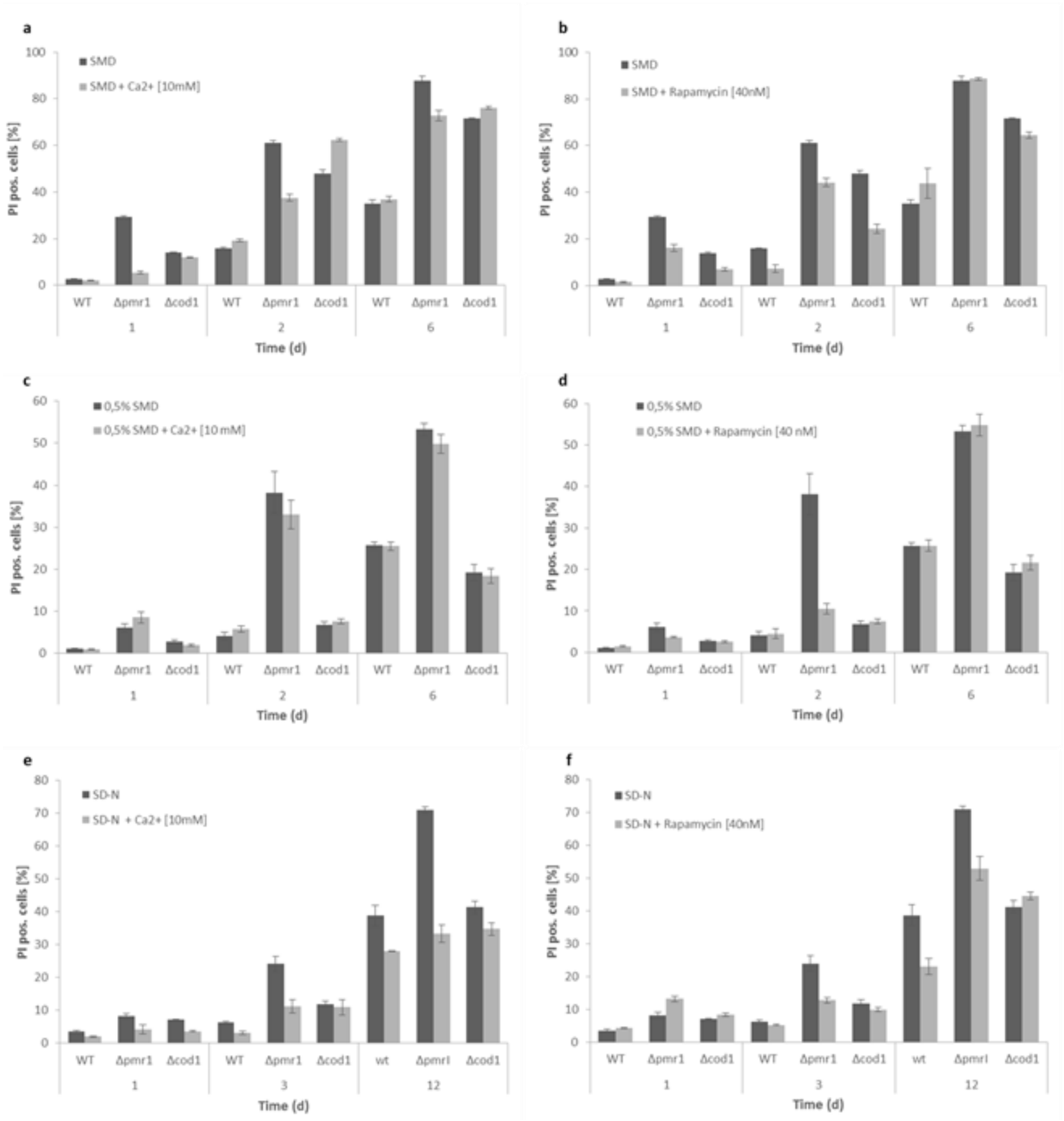

Figure 14: Cell death of WT, Δpmr1 and Δcod1 yeast cells is influenced by energy and nitrogen sources and by calcium and rapamycin treatment. *Age-related cell death (as indicated by PI pos. cells) is analyzed by flow cytometry. WT, Δpmr1 and Δcod1 cell were aged in different liquid cultures: (a) SMD containing 2% glucose with (+10 mM Ca^{2+}) and without Ca^{2+} addition. (b) SMD containing 2% glucose with (40 nM Rapamycin) and without rapamycin treatment. (c) SMD containing 0,5% glucose with (+10 mM Ca^{2+}) and without further adding of Ca^{2+}. (d) SMD containing 0,5% glucose with (40 nM Rapamycin) and without rapamycin treatment. (e-f) Cells were shifted after 6h in SMD or SMD with pre-treatments (10 mM Ca^{2+} or 40 nM rapamycin) on nitrogen starvation media with and without addition of (e) 10 mM Ca^{2+} and (f) 40 nM Rapamycin. n=4*

3.10 Nitrogen starvation with Ca^{2+} treatment completely rescues *Δpmr1* cells

As already shown in Figure 10, nitrogen starvation reduced *PMR1* deletion induced lethality. Pre-treatment with Ca^{2+} decreased cytosolic calcium levels in *Δpmr1* strains compared to its WT background (Figure 11).

It has been demonstrated that addition of calcium as well as rapamycin influenced viability of yeast cells (Figure 14). In order to verify that increased cytosolic Ca^{2+} levels correlates with toxicity, flow cytometry experiments with calcium pre-treated cells were performed, to measure age-induced cell death (quantified by PI pos. cells).

Calcium pre-treatment under nitrogen starvation conditions rescues *PMR1* deletion mutants compared to untreated cells. While, untreated *Δpmr1* cells show 70% of PI pos. cells, mortality rate declined with Ca^{2+} treatment to 33% on the twelfth day.

In summary: Nitrogen starvation with Ca^{2+} pre-treatment rescues *PMR1* deletion mutants back to wild type level during chronological ageing.

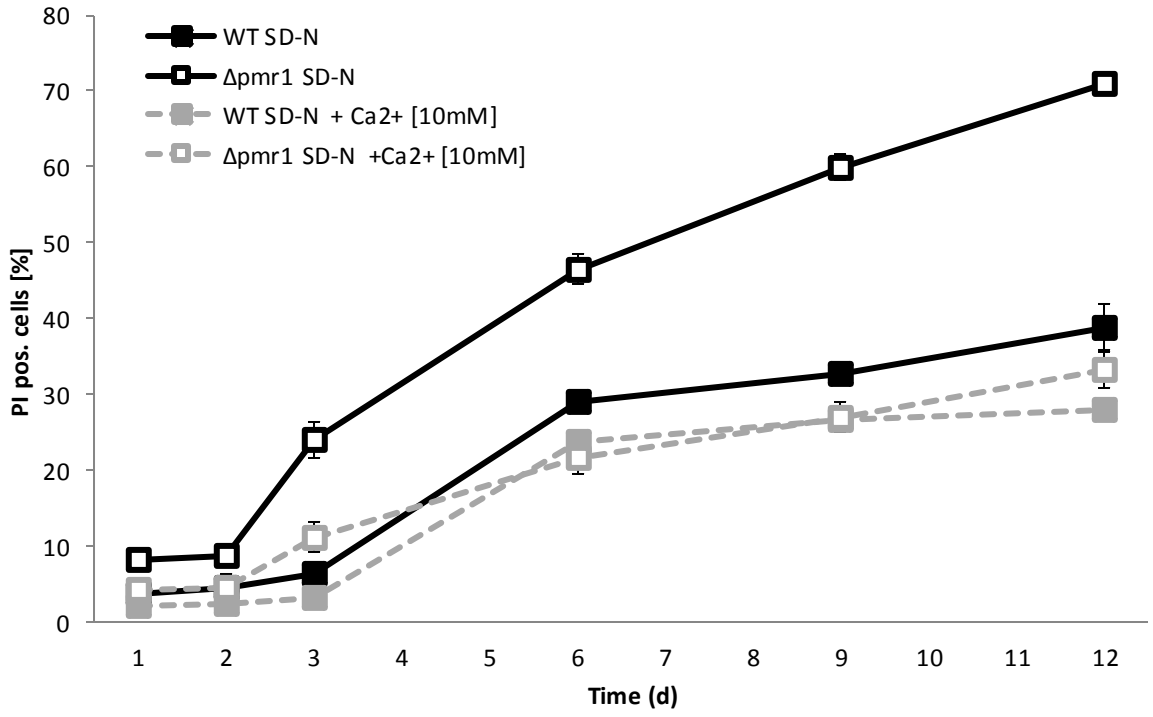

Figure 15: A combination between nitrogen starvation and Ca^{2+} pre-treatment completely rescues Δpmr1 induced toxicity. *WT and Δpmr1 cells with and without further Ca^{2+} treatment inoculated in nitrogen starvation media. Flow cytometry of age-associated cell death, measured by numbers of propidium iodid (PI) positive cells in cultures. n=3-4*

3.11 Atg8 levels are decreased in *Δpmr1* cells

Earlier Atg8-GFP-liberation assays have shown that *PMR1* knockouts cells were not deficient to perform autophagy under nitrogen starvation conditions, but lacking of Pmr1 resulted in downregulated autophagy during growth in standard minimal conditions (SMD containing 2% glucose).

It is well known that limited intake of energy increases lifespan, leads to resistance to oxidative stress and lower macromolecular damage. This dietary manipulation is designated as caloric restriction [85,86]. Therefore we used minimal media (SMD) containing 0,5% glucose instead of 2%.

We performed GFP-liberation assays to verify if caloric restriction conditions differently impacts autophagy induction and autophagic flux of *Δpmr1* and WT cells.

At indicated time points immunoblot analyses of GFP-tagged Atg8 WT and *Δpmr1* yeast cells, grown in caloric restriction conditions were executed. Specific antibodies against GFP and GAPDH as loading control were used.

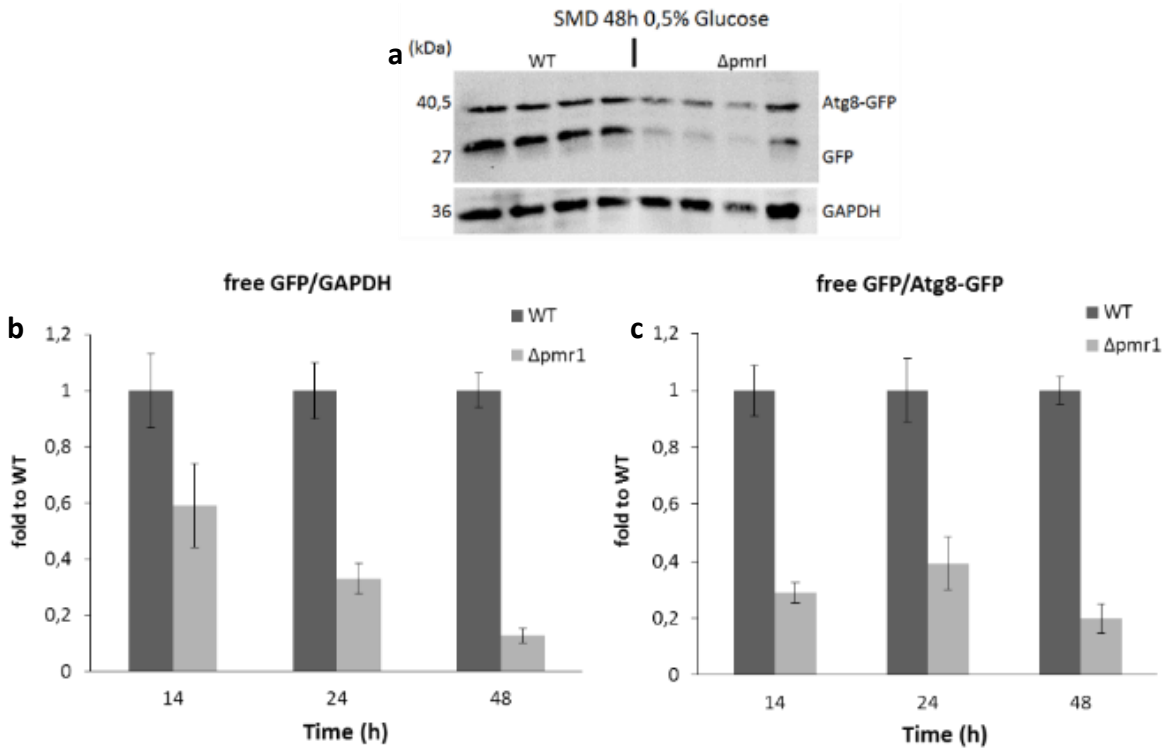

Figure 16: Caloric restriction decreases autophagy induction as well as autophagic flux in PMR1 deletion cells. *Blots were inoculated with specific antibodies against GFP (GFP-tagged Atg8 respectively) and against GAPDH as loading control. (a) Representative immunoblot analysis of GPF-tagged Atg8 cells (WT and Δpmr1) inoculates for 48h. Determination of autophagy levels of WT and Δpmr1 by GFP-liberation assays at indicated time points. Evaluated by ratio of (b) free GFP/GAPDH and (c) free GFP/Atg8-GFP. n=11-16*

A representative immunoblot is figured and the quantification was evaluated by ratio: free GFP/GAPDH and free GFP/Atg8-GFP (Figure 16).

PMR1 deletion cells show massively decreased autophagy levels compared to its wild type background strain. Total GFP levels as well as the turnover of Atg8-GFP to GFP was significantly reduced.

This data indicate that caloric restriction decreases autophagy induction as well as autophagic flux in *PMR1* deletion mutants.

We demonstrated that deletion of *PMR1* caused reduced autophagy and induced lethality when grown in standard SMD media.

We next asked if caloric restriction influences survival of cells. And could caloric restriction rescue the lethal phenotype induced by deletion of *PMR1*?

3.12 Caloric restriction decreases PI+ cells

We have found that cells lacking Pmr1 show reduced viability compared to WT cells grown in standard minimal media (SMD). The question has been raised if caloric restriction rescues toxicity caused by *PMR1* knockout.

Determination of survival during chronological aging was performed by clonogenic survival plating and lethality by flow cytometric quantification of PI pos. cells. Wild type and *Δpmr1* cells grown in standard minimal media (SMD containing 2% glucose) were compared with caloric restriction conditions (SMD containing 0,5% glucose).

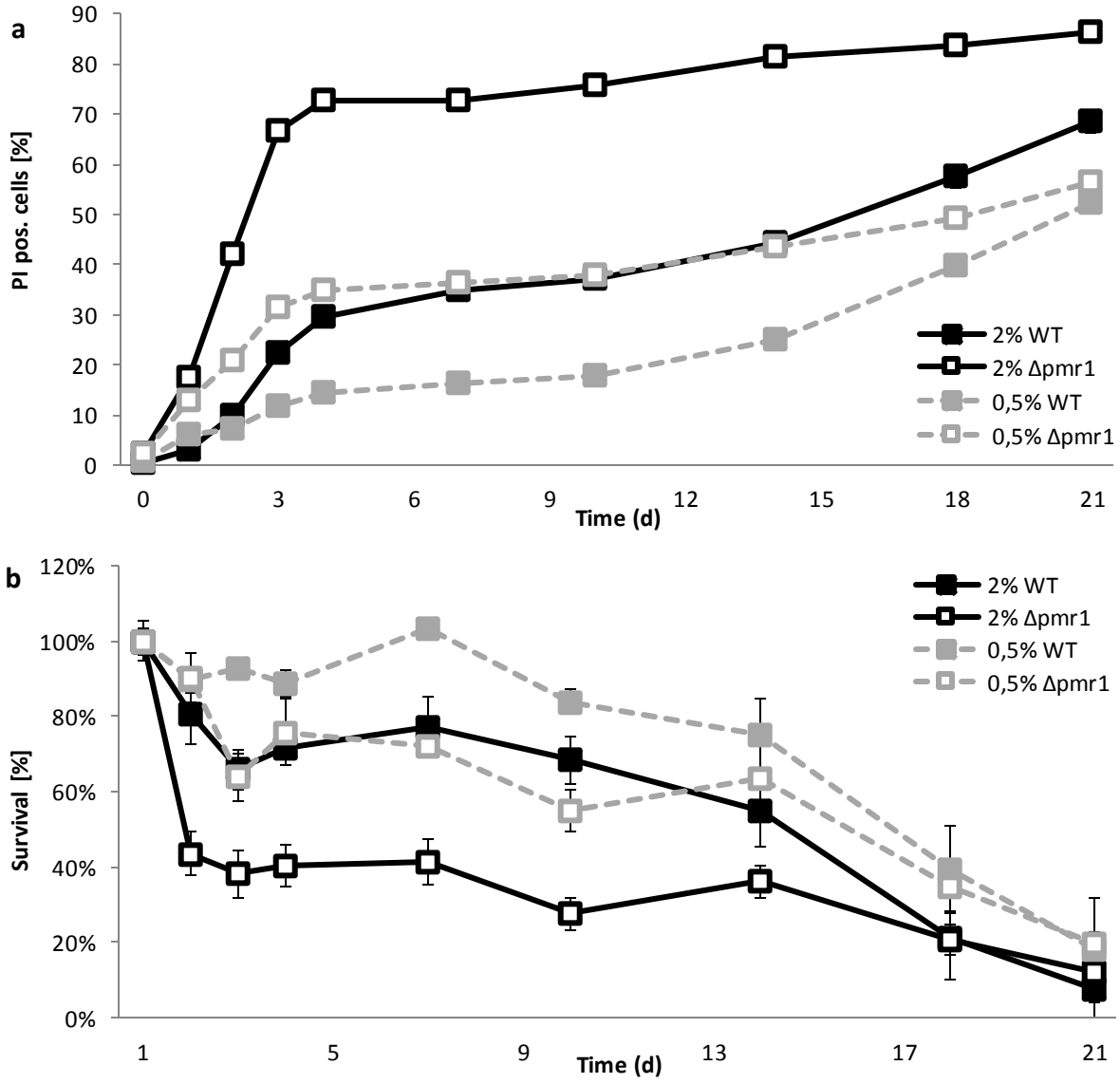

Figure 17: Caloric restriction rescues WT cells as well as PMR1 deletion mutants. *Wild type and Δpmr1 cells grown in standard minimal media (SMD containing 2% glucose) were compared with caloric restriction conditions (SMD containing 0,5% glucose). (a) PI pos. cells were analyzed by flow cytometry to detect age-related cell death, n=6. (b) Survival determinations were performed by clonogenic survival plating on YPD agar plates, n=5-6.*

As seen in Figure 17, both assays indicate that caloric restriction rescued WT cells as well as *PMR1* deletion mutants. Lower concentration of sugar has a far greater effect on mutant cells compared to its WT background.

The results demonstrate that PI staining correlates with cell death. Living cells were reversely detected by chronological plate assay.

It has been shown that caloric restriction reduced the toxic phenotype of *Δpmr1* cells. But GFP-liberation assays indicate that this didn't correlate with induction of autophagy.

On the basis of these results a possibility to reverse these effects was searched.

3.13 FK506 can restore autophagy deficiency in *Δpmr1* cells

Calcineurin is involved in transcriptional regulation and is activated by intracellular calcium[69-72]. It is proposed that activated calcineurin inhibits growth of yeast cells[73]. It has been published that calcineurin-calmodulin function is inhibited by FK506 through development of a drug-dependent complex[74,75].

We have shown that lacking of Pmr1 caused elevated Ca^{2+} levels and we know that calcineurin is activated by calcium.

We next asked if higher calcium levels and may enhanced activation of calcineurin, which in turn might influence autophagy in yeast. In order to clarify this, we used FK506 for calcineurin inhibition and performed GFP-liberation assays for quantification of autophagy levels.

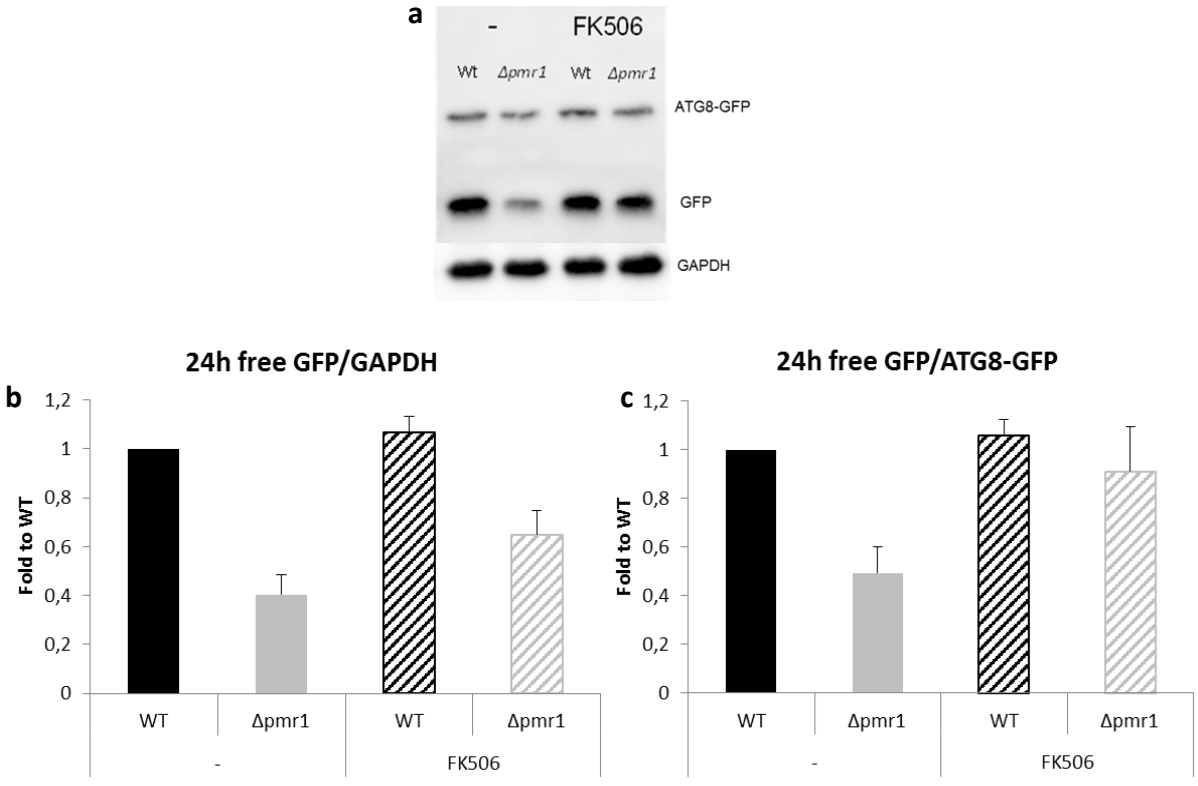

Figure 18: Treatment with FK506 elevates autophagy levels in Δpmr1 cells. *Immunoblot analysis of WT and Δpmr1 cells grown under caloric restriction conditions with and without FK506 treatment for 24h. Immunoblots were performed with antibodies against GFP and GAPDH (as loading control). (a) Representative immunoblots of WT and Δpmr1 cells and autophagic flux determining by Atg8GFP-liberation assay. Ratio of (b) free GFP/GAPDH and (c) free GFP/Atg8-GFP of WT and Δpmr1 were evaluated. n=8. Experiments carried out by Lukas Habernig.*

Cells were inoculated into two different growth media. On the one hand minimal growth media, containing 0,5% glucose. This medium was chosen because of the great differences in autophagy induction between WT and *PMR1* deletion cells (Figure 16). On the other hand cells were inoculated in SMD (0,5% glucose) with FK506 (0,5 µM) subsequently added to the media.

Autophagic flux was detected by immunoblot analysis using antibodies against GFP and GAPDH. Figure 18 shows one representative blot and two quantifications: free GFP/GAPDH and free GFP/Atg8-GFP.

These data confirm that lacking of *PMR1* caused decreased autophagy levels compared to its wild type background strain under caloric restriction conditions. But treatment of cells with FK506 elevated autophagy levels in *PMR1* knock out strains. Especially the autophagic flux of *Δpmr1* cells could restored by calcineurin inhibition

These data suggest that increased levels of calcium may induce excessive activation of calcineurin and downregulation of autophagy.

4. Discussion

In yeast, *PMR1* encodes the main Golgi Ca^{2+}-ATPase[43]. Mutations of the human homologous protein ATP2C1 leads to the skin disorder named Hailey–Hailey disease[57].

The role of calcium as second messenger is conserved from yeast to humans[28]. Alterations in these Ca^{2+} homeostatic mechanisms can cause numerous diseases[31], for example cardiac hypertrophy as well as sudden cardiac death[34–36], neurodegenerative diseases like Alzheimer disease and Huntington[37–39] and cancer[40,41]. It has been published that intracellular Ca^{2+} signaling can stimulate or abrogate autophagy[29].

Autophagy is necessary for degradation of cytoplasmic materials, including protein aggregates and organelles. An important tasks of autophagy is to ensure the recycling of cellular components and cell homeostasis[4,5].

Age-related cell death of WT cells compared to cells lacking *PMR1* was observed. Lethality was detected by flow cytometric quantification of propidium iodide (PI) positive cells over a time period of 21 days. We could show that *PMR1* deletion mutants exhibited lower viability compared to wild type cells. The genes *PMR1* and *HUR1* partly overlap in yeast chromosome[50,51]. Our data indicates that lacking functional Hur1 does not influence viability of *PMR1* knockout strains.

Autophagy levels were determined using Atg8-GFP-liberation assays. These data suggest that cells lacking Pmr1 exhibit downregulated autophagy under standard minimal growth and caloric restriction conditions. These reduction of autophagy could be partly restored by nitrogen starvation. This indicates that *Δpmr1* cells are not deficient to perform autophagy.

Previous studies showed that *PMR1* deletion causes elevated $[Ca^{2+}]_i$ levels and changed Ca^{2+} flux[47]. We confirmed increased cytosolic as well as total Ca^{2+} levels in *Δpmr1* cells.

We also performed experiments to monitor the cellular response to high external Ca^{2+}. Cells were treated with a high dosage of Ca^{2+} and transient $[Ca^{2+}]_{cyt}$ response was observed.

Wild type cells could react promptly to high doses of calcium after treatment. Cytosolic calcium levels of cells lacking Pmr1 were two-times higher after Ca^{2+} treatment and a decrease of $[Ca^{2+}]_{cyt}$ took longer compared to WT cells.

Surprisingly when *Δpmr1* cells were pre-treated with 10 mM $CaCl_2$ their Ca^{2+} response improved. With previous calcium treatment, cells lacking Pmr1 showed lower basal cytosolic Ca^{2+} levels and were less sensitive to high doses of Ca^{2+}.

We have observed that lacking of *PMR1* caused decreased viability and reduced autophagy levels compared to wild type cells grown in standard SMD media. It is known that lack of nitrogen sources induce autophagy and promote longevity[6].

Our data indicates that nitrogen starvation induced autophagy and reduced lethality of *Δpmr1*. A combination between nitrogen starvation and Ca^{2+} pre-treatment completely rescued *Δpmr1* induced toxicity.

According to the literature, calcineurin, a Ca^{2+}-responsive regulator of transcription is inhibited by compound FK506[69–72,74,75].

We demonstrated that caloric restriction massively decreased autophagy levels in cells lacking *PMR1.* Inhibition of calcineurin by FK506 could restore autophagy defects of *Δpmr1* cells.

In summary, enhancement of calcium levels and lower viability of *PMR1* deletion mutants were partly prevented by Ca^{2+} pre-treatment. Calcineurin inhibition restored autophagy defects of *Δpmr1* cells.

These data suggest that deletion of *PMR1* resulted in increased levels of calcium. This may induce age-related lethality, excessive activation of calcineurin and downregulation of autophagy.

Our results might even help to provide new insights into the connection between calcium homeostasis and autophagy. This can be an important fundament for developing of new therapeutic strategies to deal with the Hailey-Hailey disease in future.

5. Abbreviations

$[Ca^{2+}]_{cyt}$	cytosolic Calcium ions
$[Ca^{2+}]_i$	intracellular Ca^{2+}
µg	microgram
µl	microliter
AMPK	AMP-activated protein kinase
AS	ammoniumsulfat
Atg	autophagy related gene
ATG8-GFP	endogenously GFP-tagged ATG8
bp	base pair
BSA	Bovine serum albumin
Ca^{2+}	calcium ions
cfu	colony forming units
CMA	chaperone mediated autophagy
C-terminal	carboxy -terminal
ddH_2O	double deionized water
DHE	dihydroethidium
DMSO	dimethyl sulfoxide
DNA	deoxyribonucleic acid
dNTP	desoxy nucleoside triphosphate
dNTPs	nucleotide triphosphates
E. coli	*Escherichia coli*
eEF2	elongation factor 2
ER	endoplasmic reticulum
Eth.	ethidium
FK506	tacrolimus
GAPDH	Glyceraldehyde 3-phosphate dehydrogenase
GFP	Green fluorescent protein
GFP- ATG8	endogenously GFP-tagged ATG8

HHD	Hailey–Hailey disease
HRP	horseradish peroxidase
IP_3R	1,4,5-Trisphosphate receptor
mg	milligram
ml	milliliter
mTOR	mammalia target of rapamycin
PI	propidium iodide
PI3IK	phosphatidylinositol-3 kinase
rlu	relative fluorescence units
ROS	reactive oxygen species
rpm	revolutions per minute
RT	room temperature
S. cerevisiae (S. c.)	*Saccharomyces cerevisiae,* yeast
SD-N	nitrogen starvation media
SMD	standard minimal media
TOR	target of rapamycin
WT	wild type (BY4741)
YNB	yeast nitrogen base

6. Attachments

YGL167C Chromosome 7 from 187316 to 190768

CATCAAGACAAGATTCTCTATTTAAAGAAGTACTTTTTTTGTTAACAGTGTGGACCCTAC
CTATCGTTATATCGAGATCTTGTTCCCTAGGCCATCGTACACTATAGCCCTTCCTTCAAG
CACTTAATAGAAAAACCTCTTTTTCTACACCATCATAATAGTGTTTGCTCGCCCCGTTCT
TTCCATTCCCATTTATAACAATACTAGTAACTATAATAATATCCTTACGACTGGGCAAGA
CAAGACGAAGCAAGGCCAGCACAGACGTAAGCTTAAGTGTAAGTAAAAGATAAGATAATT
ATGAGTGACAATCCATTTAATGCGAGTCTTCTTGACGAGGACTCAAACCGTGAGAGAGAA
ATACTAGATGCCACAGCAGAGGCCCTTTCGAAACCAAGCCCTTCTTTAGAGTATTGTACT
TTATCCGTGGACGAAGCTCTAGAAAAACTGGACACTGACAAAAACGGTGGTTTACGATCA
TCTAACGAGGCCAACAATAGGAGATCACTTTATGGCCCCAATGAAATAACCGTAGAAGAT
GATGAAAGTCTTTTCAAGAAGTTCTTGTCAAATTTCATTGAGGATCGAATGATTCTACTT
TTAATAGGATCCGCAGTGGTCTCTCTTTTTATGGGTAACATTGATGATGCTGTTAGTATC
ACACTGGCCATTTTCATAGTTGTCACTGTCGGTTTTGTCCAAGAATATAGGTCTGAAAAA
TCTCTAGAAGCGTTGAATAAATTGGTTCCTGCTGAATGTCACTTAATGAGATGTGGTCAA
GAGAGTCATGTACTGGCTTCCACCTTGGTTCCTGGTGATTTAGTGCACTTCAGAATAGGT
GACAGAATCCCCGCAGACATTAGAATTATTGAAGCAATCGATTTATCCATCGATGAAAGT
AATTTAACTGGTGAAAATGAACCGGTACATAAAACCTCACAAACGATCGAAAAATCTTCC
TTTAACGATCAGCCTAATTCAATTGTACCGATTTCTGAGAGATCTTGTATAGCTTATATG
GGTACATTAGTCAAGGAAGGTCATGGTAAGGGTATCGTCGTAGGAACAGGTACAAACACA
TCCTTTGGTGCCGTTTTTGAAATGATGAATAATATTGAAAAACCGAAGACTCCATTGCAG
TTAACAATGGACAAATTGGGAAAGGACTTGTCACTGGTTAGCTTCATAGTTATTGGTATG
ATTTGTTTAGTTGGTATCATACAAGGTAGATCTTGGTTAGAAATGTTCCAAATATCGGTA
TCCTTAGCGGTTGCTGCTATTCCAGAAGGGTTACCAATTATTGTCACTGTTACTTTGGCA
TTGGGTGTTCTGAGAATGGCCAAGCGTAAAGCCATCGTGAGAAGGTTACCAAGTGTCGAA
ACTTTAGGCTCTGTCAACGTTATCTGCTCCGACAAAACAGGTACACTAACCTCAAACCAC
ATGACCGTATCTAAACTTTGGTGCTTGGACAGTATGTCCAATAAGCTAAACGTCCTCTCA
TTAGACAAAAATAAGAAGACTAAAAATTCTAATGGAAATTTGAAAAACTATTTGACTGAA
GACGTTAGGGAAACTCTAACTATCGGTAATCTCTGTAATAATGCATCTTTCTCTCAAGAA
CATGCCATATTTCTGGGAAATCCTACTGATGTAGCTCTTTTAGAGCAATTGGCAAACTTT
GAAATGCCTGATATCAGAAACACCGTTCAAAAAGTTCAGGAACTTCCATTTAACTCGAAA
AGAAAATTAATGGCAACCAAGATTCTCAACCCTGTCGACAATAAGTGTACAGTTTATGTT
AAAGGTGCATTTGAAAGAATTCTTGAGTACTCCACAAGTTATTTGAAATCAAAGGGTAAA
AAAACTGAAAAGTTGACTGAAGCCCAAAAAGCTACGATAAATGAGTGCGCAAATTCTATG
GCATCTGAAGGTTTGCGTGTCTTTGGATTTGCTAAACTAACTTTGTCTGATTCATCAACT
CCTCTAACCGAAGACCTAATCAAAGATTTAACCTTTACTGGTTTAATCGGTATGAATGAC
CCACCAAGACCGAACGTTAAATTTGCCATCGAACAATTACTACAAGGTGGTGTCCATATT
ATTATGATCACTGGTGATTCTGAGAATACCGCAGTAAACATTGCAAAACAAATTGGTATT
CCAGTTATTGATCCAAAGCTTTCCGTTTTATCCGGTGATAAATTAGATGAAATGTCAGAT
GATCAACTGGCCAATGTCATCGACCACGTTAATATTTTTGCTCGTGCTACGCCTGAGCAT
AAGTTAAACATTGTTCGTGCATTAAGAAAGAGGGGTGATGTGGTAGCAATGACTGGTGAT
GGTGTTAACGACGCTCCTGCGTTGAAACTTTCAGATATTGGTGTTTCTATGGGTAGAATT
GGTACAGATGTAGCCAAAGAAGCCTCAGATATGGTCTTAACTGATGATGACTTCAGTACT
ATTTTAACTGCCATTGAAGAGGGTAAAGGTATCTTTAATAATATTCAGAATTTCCTGACT
TTTCAATTGTCTACTTCTGTTGCCGCACTATCATTAGTTGCACTATCTACAGCGTTTAAA
CTACCCAATCCACTGAACGCAATGCAAATTCTTTGGATAAATATTTTAATGGATGGGCCA
CCAGCTCAATCCTTAGGTGTGGAACCTGTTGATCATGAAGTTATGAAAAAACCTCCAAGA
AAACGTACCGATAAAATTTTGACCCATGATGTAATGAAACGTTTACTAACCACCGCGGCC
TGTATCATCGTTGGGACAGTTTACATTTTTGTTAAAGAGATGGCCGAAGATGGTAAAGTA
ACTGCTAGAGATACTACTATGACATTTACTTGTTTTGTTTTTTTTGATATGTTTAATGCT
TTGGCCTGCAGACATAACACAAAGTCAATCTTCGAAATCGGCTTTTTCACGAACAAAATG
TTCAACTACGCCGTTGGACTGTCTCTGTTAGGTCAAATGTGCGCTATATATATACCATTT
TTCCAAAGTATCTTTAAAACTGAGAAACTTGGTATCTCTGATATACTATTGTTATTGCTC
ATCAGCAGTAGCGTTTTCATCGTTGATGAATTGAGAAAATTGTGGACGAGGAAAAAGAAT
GAAGAAGACTCAACGTATTTCTCAAATGTTTGATATGTCACATTTTGTGCTTTTATCGTT
TTTCCTTCCTTCCCTTTATCTTTCATGAGGACGCCCAACCCTATTGAGGTAAATGTACTA
ATTAATGGGAACATATGTAGATGTATATATGTACATATATTTACAACGGATACTAAGATA
AACATGTATGGGCGACTTTTCGTATATACAAAGCAATATAAAATTTTATTCTTTCCTTCT
TTTTCCGGACTAGATATAAAATCTCCGTAATCAGTGGTTATGATTTTCAAAAGTTAATCA
CAGTTTTATTTAAAACTGTATACAATTATTTGC

PMR1

***HUR1* overlapping region**

Primers:

Pmr1KO_se

CAGCACAGACGTAAGCTTAAGTGTAAGTAAAAGATAAGATAATCAGCTGAAGCTTCGTACGC

43 bp; (Tm 60°C)

Pmr1KO_an1

ATGTGACATATCAAACATTTGAGAAATACGTTGAGTCTTCTTCGCATAGGCCACTAGTGGAT

CTG

43 bp; (Tm 64°C)

Pmr1KO_an2

TAACAGAGACAGTCCAACGGCGTAGTTGAACATTTTGTTGCATAGGCCACTAGTGGATCTG

39 bp; Tm 64°C

Pmr1ctrlse1

CTAGGCCATCGTACACTATAGC

Tm 59,8°C

Pmr1_ctrlan

GCTTTGTATATACGAAAAGTCGCC

Tm 57,8°C

7. References

1. Goffeau, A. *et al.* Life with 6000 genes. *Science* **274,** 546, 563–567 (1996).

2. Duina, A. A., Miller, M. E. & Keeney, J. B. Budding Yeast for Budding Geneticists: A Primer on the Saccharomyces cerevisiae Model System. *Genetics* **197,** 33–48 (2014).

3. Longo, V. D., Shadel, G. S., Kaeberlein, M. & Kennedy, B. Replicative and Chronological Aging in Saccharomyces cerevisiae. *Cell Metabolism* **16,** 18–31 (2012).

4. Ravikumar, B. *et al.* Regulation of Mammalian Autophagy in Physiology and Pathophysiology. *Physiological Reviews* **90,** 1383–1435 (2010).

5. Reggiori, F. & Klionsky, D. J. Autophagic Processes in Yeast: Mechanism, Machinery and Regulation. *Genetics* **194,** 341–361 (2013).

6. Markaki, M. & Tavernarakis, N. Metabolic Control by Target of Rapamycin and Autophagy during Ageing - A Mini-Review. *Gerontology* **59,** 340–348 (2013).

7. Kapahi, P. *et al.* With TOR less is more: a key role for the conserved nutrient sensing TOR pathway in aging. *Cell Metab* **11,** 453–465 (2010).

8. Rabinowitz, J. D. & White, E. Autophagy and Metabolism. *Science* **330,** 1344–1348 (2010).

9. Mizushima, N. The role of the Atg1/ULK1 complex in autophagy regulation. *Current Opinion in Cell Biology* **22,** 132–139 (2010).

10. Sonenberg, N. & Hinnebusch, A. G. Regulation of Translation Initiation in Eukaryotes: Mechanisms and Biological Targets. *Cell* **136,** 731–745 (2009).

11. Hay, N. & Sonenberg, N. Upstream and downstream of mTOR. *Genes Dev.* **18,** 1926–1945 (2004).

12. Kaul, G., Pattan, G. & Rafeequi, T. Eukaryotic elongation factor-2 (eEF2): its regulation and peptide chain elongation. *Cell Biochem. Funct.* **29,** 227–234 (2011).

13. Hizli, A. A. *et al.* Phosphorylation of Eukaryotic Elongation Factor 2 (eEF2) by Cyclin A–Cyclin-Dependent Kinase 2 Regulates Its Inhibition by eEF2 Kinase. *Mol Cell Biol* **33,** 596–604 (2013).

14. Browne, G. J. & Proud, C. G. Regulation of peptide-chain elongation in mammalian cells. *Eur. J. Biochem.* **269,** 5360–5368 (2002).

15. Ahlberg, J. & Glaumann, H. Uptake--microautophagy--and degradation of exogenous proteins by isolated rat liver lysosomes. Effects of pH, ATP, and inhibitors of proteolysis. *Exp. Mol. Pathol.* **42,** 78–88 (1985).

16. Martinez-Vicente, M. Autophagy in neurodegenerative diseases: From pathogenic dysfunction to therapeutic modulation. *Seminars in Cell & Developmental Biology* **40,** 115–126 (2015).

17. Cuervo, A. M., Knecht, E., Terlecky, S. R. & Dice, J. F. Activation of a selective pathway of lysosomal proteolysis in rat liver by prolonged starvation. *American Journal of Physiology - Cell Physiology* **269,** C1200–C1208 (1995).

18. Kiffin, R., Christian, C., Knecht, E. & Cuervo, A. M. Activation of Chaperone-mediated Autophagy during Oxidative Stress. *Mol. Biol. Cell* **15,** 4829–4840 (2004).

19. Massey, A. C., Zhang, C. & Cuervo, A. M. Chaperone-mediated autophagy in aging and disease. *Curr. Top. Dev. Biol.* **73,** 205–235 (2006).

20. Sooparb, S., Price, S. R., Shaoguang, J. & Franch, H. A. Suppression of chaperone-mediated autophagy in the renal cortex during acute diabetes mellitus. *Kidney Int.* **65,** 2135–2144 (2004).

21. Cuervo, A. M., Stefanis, L., Fredenburg, R., Lansbury, P. T. & Sulzer, D. Impaired degradation of mutant alpha-synuclein by chaperone-mediated autophagy. *Science* **305,** 1292–1295 (2004).

22. Vellai, T. Autophagy genes and ageing. *Cell Death and Differentiation* **16,** 94–102 (2009).

23. Levine, B. & Klionsky, D. J. Development by Self-Digestion. *Developmental Cell* **6,** 463–477 (2004).

24. Suzuki, K. & Ohsumi, Y. Molecular machinery of autophagosome formation in yeast, Saccharomyces cerevisiae. *FEBS Letters* **581,** 2156–2161 (2007).

25. Kirisako, T. *et al.* Formation Process of Autophagosome Is Traced with Apg8/Aut7p in Yeast. *J Cell Biol* **147,** 435–446 (1999).

26. Klionsky, D. J. *et al.* Guidelines for the use and interpretation of assays for monitoring autophagy. *Autophagy* **8,** 445–544 (2012).

27. Klionsky, D. J., Cuervo, A. M. & Seglen, P. O. Methods for Monitoring Autophagy from Yeast to Human. *Autophagy* **3,** 181–206 (2007).

28. Harr, M. W. & Distelhorst, C. W. Apoptosis and autophagy: decoding calcium signals that mediate life or death. *Cold Spring Harb Perspect Biol* **2,** a005579 (2010).

29. Decuypere, J.-P., Bultynck, G. & Parys, J. B. A dual role for Ca(2+) in autophagy regulation. *Cell Calcium* **50,** 242–250 (2011).

30. Dunn, T., Gable, K. & Beeler, T. Regulation of cellular Ca2+ by yeast vacuoles. *J. Biol. Chem.* **269,** 7273–7278 (1994).

31. Sammels, E., Parys, J. B., Missiaen, L., De Smedt, H. & Bultynck, G. Intracellular Ca2+ storage in health and disease: a dynamic equilibrium. *Cell Calcium* **47,** 297–314 (2010).

32. Berridge, M. J. The endoplasmic reticulum: a multifunctional signaling organelle. *Cell Calcium* **32,** 235–249 (2002).

33. Clapham, D. E. Calcium Signaling. *Cell* **131,** 1047–1058 (2007).

34. Kranias, E. G. & Bers, D. M. Calcium and cardiomyopathies. *Subcell. Biochem.* **45,** 523–537 (2007).

35. Hamada, T., Gangopadhyay, J. P., Mandl, A., Erhardt, P. & Ikemoto, N. Defective regulation of the ryanodine receptor induces hypertrophy in cardiomyocytes. *Biochemical and Biophysical Research Communications* **380,** 493–497 (2009).

36. Lehnart, S. E. *et al.* Leaky Ca2+ release channel/ryanodine receptor 2 causes seizures and sudden cardiac death in mice. *J. Clin. Invest.* **118,** 2230–2245 (2008).

37. LaFerla, F. M. Calcium dyshomeostasis and intracellular signalling in alzheimer's disease. *Nature Reviews Neuroscience* **3,** 862–872 (2002).

38. Cheung, K.-H. *et al.* Mechanism of Ca2+ disruption in Alzheimer's disease by presenilin regulation of InsP3 receptor channel gating. *Neuron* **58,** 871–883 (2008).

39. Bezprozvanny, I. & Mattson, M. P. Neuronal calcium mishandling and the pathogenesis of Alzheimer's disease. *Trends Neurosci.* **31,** 454–463 (2008).

40. Bergner, A. & Huber, R. M. Regulation of the endoplasmic reticulum Ca(2+)-store in cancer. *Anticancer Agents Med Chem* **8,** 705–709 (2008).

41. Monteith, G. R., McAndrew, D., Faddy, H. M. & Roberts-Thomson, S. J. Calcium and cancer: targeting Ca2+ transport. *Nat. Rev. Cancer* **7,** 519–530 (2007).

42. Rudolph, H. K. *et al.* The yeast secretory pathway is perturbed by mutations in PMR1, a member of a Ca2+ ATPase family. *Cell* **58,** 133–145 (1989).

43. Marchi, V., Sorin, A., Wei, Y. & Rao, R. Induction of vacuolar Ca2+-ATPase and H+/Ca2+ exchange activity in yeast mutants lacking Pmr1, the Golgi Ca2+-ATPase. *FEBS Lett.* **454,** 181–186 (1999).

44. Strayle, J., Pozzan, T. & Rudolph, H. K. Steady-state free Ca2+ in the yeast endoplasmic reticulum reaches only 10 µM and is mainly controlled by the secretory pathway pump Pmr1. *The EMBO Journal* **18,** 4733–4743 (1999).

45. Locke, E. G., Bonilla, M., Liang, L., Takita, Y. & Cunningham, K. W. A Homolog of Voltage-Gated Ca2+ Channels Stimulated by Depletion of Secretory Ca2+ in Yeast. Molecular and Cellular Biology 20, 6686–6694 (2000).

46. Lapinskas, P. J., Cunningham, K. W., Liu, X. F., Fink, G. R. & Culotta, V. C. Mutations in PMR1 suppress oxidative damage in yeast cells lacking superoxide dismutase. *Mol. Cell. Biol.* **15,** 1382–1388 (1995).

47. Halachmi, D. & Eilam, Y. Elevated cytosolic free Ca2+ concentrations and massive Ca2+ accumulation within vacuoles, in yeast mutant lacking PMR1, a homolog of Ca2+-ATPase. *FEBS Letters* **392,** 194–200 (1996).

48. Büttner, S. *et al.* The Ca2+/Mn2+ ion-pump PMR1 links elevation of cytosolic Ca(2+) levels to α-synuclein toxicity in Parkinson's disease models. *Cell Death Differ.* **20,** 465–477 (2013).

49. Devasahayam, G., Ritz, D., Helliwell, S. B., Burke, D. J. & Sturgill, T. W. Pmr1, a Golgi Ca2+/Mn2+-ATPase, is a regulator of the target of rapamycin (TOR) signaling pathway in yeast. *Proceedings of the National Academy of Sciences* **103,** 17840–17845 (2006).

50. HUR1 | SGD. at <http://www.yeastgenome.org/locus/S000003136/overview> (28.06.2015).

51. PMR1 Sequence | SGD. at <http://www.yeastgenome.org/locus/S000003135/sequence> (28.06.2015).

52. Zewail, A. *et al.* Novel functions of the phosphatidylinositol metabolic pathway discovered by a chemical genomics screen with wortmannin. *Proceedings of the National Academy of Sciences* **100,** 3345–3350 (2003).

53. Suzuki, C. & Shimma, Y. P-type ATPase spf1 mutants show a novel resistance mechanism for the killer toxin SMKT. *Molecular Microbiology* **32,** 813–823 (1999).

54. Cronin, S. R. Regulation of HMG-CoA Reductase Degradation Requires the P-Type ATPase Cod1p/Spf1p. *The Journal of Cell Biology* **148,** 915–924 (2000).

55. Cronin, S. R. Cod1p/Spf1p is a P-type ATPase involved in ER function and Ca2+ homeostasis. *The Journal of Cell Biology* **157,** 1017–1028 (2002).

56. Hailey, H. FAMILIAL BENIGN CHRONIC PEMPHIGUS. *Archives of Dermatology* **39,** 679 (1939).

57. Sudbrak, R. Hailey-Hailey disease is caused by mutations in ATP2C1 encoding a novel Ca2+ pump. *Human Molecular Genetics* **9,** 1131–1140 (2000).

58. Behne, M. J. *et al.* Human Keratinocyte ATP2C1 Localizes to the Golgi and Controls Golgi Ca2+ Stores. *Journal of Investigative Dermatology* **121,** 688–694 (2003).

59. Aronchik, I. *et al.* Actin Reorganization Is Abnormal and Cellular ATP Is Decreased in Hailey-Hailey Keratinocytes. *Journal of Investigative Dermatology* **121,** 681–687 (2003).

60. Hu, Z. *et al.* Mutations in ATP2C1, encoding a calcium pump, cause Hailey-Hailey disease. *Nat Genet* **24,** 61–65 (2000).

61. Szigeti, R. & Kellermayer, R. Hailey-Hailey Disease and Calcium: Lessons from Yeast. *Journal of Investigative Dermatology* **123,** 1195–1196 (2004).

62. Voisset, C., García-Rodríguez, N., Birkmire, A., Blondel, M. & Wellinger, R. E. Using yeast to model calcium-related diseases: Example of the Hailey–Hailey disease. *Biochimica et Biophysica Acta (BBA) - Molecular Cell Research* **1843,** 2315–2321 (2014).

63. Ikeda, S., Suga, Y. & Ogawa, H. Successful management of Hailey-Hailey disease with potent topical steroid ointment. *Journal of Dermatological Science* **5,** 205–211 (1993).

64. Burge, S. M. Hailey–Hailey disease: the clinical features, response to treatment and prognosis. *British Journal of Dermatology* **126,** 275–282 (1992).

65. Rabeni, E. J. & Cunningham, N. M. Effective treatment of Hailey-Hailey disease with topical tacrolimus? *Journal of the American Academy of Dermatology* **47,** 797–798 (2002).

66. Iida, H., Nakamura, H., Ono, T., Okumura, M. S. & Anraku, Y. MID1, a novel Saccharomyces cerevisiae gene encoding a plasma membrane protein, is required for Ca2+ influx and mating. *Mol. Cell. Biol.* **14,** 8259–8271 (1994).

67. Fischer, M. *et al.* The Saccharomyces cerevisiae CCH1 gene is involved in calcium influx and mating. *FEBS Lett.* **419,** 259–262 (1997).

68. Miseta, A., Kellermayer, R., Aiello, D. P., Fu, L. W. & Bedwell, D. M. The vacuolar Ca2+/H+ exchanger Vcx1p/Hum1p tightly controls cytosolic Ca2+ levels in S-cerevisiae. *FEBS Lett.* **451,** 132–136 (1999).

69. Stathopoulos, A. M. & Cyert, M. S. Calcineurin acts through the CRZ1/TCN1-encoded transcription factor to regulate gene expression in yeast. *Genes & Development* **11,** 3432–3444 (1997).

70. Matheos, D. P., Kingsbury, T. J., Ahsan, U. S. & Cunningham, K. W. Tcn1p/Crz1p, a calcineurin-dependent transcription factor that differentially regulates gene expression in Saccharomyces cerevisiae. *Genes & Development* **11,** 3445–3458 (1997).

71. Klee, C. & Cohen, P. *The calmodulin-regulated protein phosphatase. in Molecular Aspects of Cellular Regulation: Calmodulin, eds Cohen P, Klee CB (Elsevier, Amsterdam)*. (1988).

72. Rusnak, F. & Mertz, P. Calcineurin: form and function. *Physiol. Rev.* **80,** 1483–1521 (2000).

73. Cunningham, K. W. & Fink, G. R. Calcineurin-dependent growth control in Saccharomyces cerevisiae mutants lacking PMC1, a homolog of plasma membrane Ca2+ ATPases. *J. Cell Biol.* **124,** 351–363 (1994).

74. Liu, J. *et al.* Calcineurin is a common target of cyclophilin-cyclosporin A and FKBP-FK506 complexes. *Cell* **66,** 807–815 (1991).

75. Cardenas, M. E. *et al.* Immunophilins interact with calcineurin in the absence of exogenous immunosuppressive ligands. *EMBO J.* **13,** 5944–5957 (1994).

76. Ton, V.-K. & Rao, R. Functional expression of heterologous proteins in yeast: insights into Ca2+ signaling and Ca2+-transporting ATPases. *AJP: Cell Physiology* **287,** C580–C589 (2004).

77. Sawada, S., Suzuki, G., Kawase, Y. & Takaku, F. Novel immunosuppressive agent, FK506. In vitro effects on the cloned T cell activation. *J. Immunol.* **139,** 1797–1803 (1987).

78. Iwasaki, K. Metabolism of tacrolimus (FK506) and recent topics in clinical pharmacokinetics. *Drug Metab. Pharmacokinet.* **22,** 328–335 (2007).

79. Eisenberg, T. *et al.* Nucleocytosolic Depletion of the Energy Metabolite Acetyl-Coenzyme A Stimulates Autophagy and Prolongs Lifespan. *Cell Metabolism* **19,** 431–444 (2014).

80. Janke, C. *et al.* A versatile toolbox for PCR-based tagging of yeast genes: new fluorescent proteins, more markers and promoter substitution cassettes. *Yeast* **21,** 947–962 (2004).

81. Davey, H. M. & Hexley, P. Red but not dead? Membranes of stressed Saccharomyces cerevisiae are permeable to propidium iodide. *Environmental Microbiology* **13,** 163–171 (2011).

82. Bradner, J. R. & Nevalainen, K. M. H. Metabolic activity in filamentous fungi can be analysed by flow cytometry. *Journal of Microbiological Methods* **54,** 193–201 (2003).

83. Ottolini, D., Calì, T. & Brini, M. in *Methods in Enzymology* (ed. Kroemer, L. G. and G.) **543,** 21–45 (Academic Press, 2014).

84. An, Z. *et al.* Autophagy is required for G_1/G_0 quiescence in response to nitrogen starvation in *Saccharomyces cerevisiae*. *Autophagy* **10,** 1702–1711 (2014).

85. Fontana, L., Partridge, L. & Longo, V. D. Extending Healthy Life Span--From Yeast to Humans. *Science* **328,** 321–326 (2010).

86. Masoro, E. J. Overview of caloric restriction and ageing. *Mechanisms of Ageing and Development* **126,** 913–922 (2005).